

---

Doctoral Dissertations

Student Theses and Dissertations

---

2011

## Surface modification of micro-fluidic devices

Zhan Gao

Follow this and additional works at: [https://scholarsmine.mst.edu/doctoral\\_dissertations](https://scholarsmine.mst.edu/doctoral_dissertations)

 Part of the [Chemical Engineering Commons](#)

Department: Chemical and Biochemical Engineering

---

### Recommended Citation

Gao, Zhan, "Surface modification of micro-fluidic devices" (2011). *Doctoral Dissertations*. 81.  
[https://scholarsmine.mst.edu/doctoral\\_dissertations/81](https://scholarsmine.mst.edu/doctoral_dissertations/81)

This thesis is brought to you by Scholars' Mine, a service of the Missouri S&T Library and Learning Resources. This work is protected by U. S. Copyright Law. Unauthorized use including reproduction for redistribution requires the permission of the copyright holder. For more information, please contact [scholarsmine@mst.edu](mailto:scholarsmine@mst.edu).

SURFACE MODIFICATION OF MICRO-FLUIDIC DEVICES

by

ZHAN GAO

A DISSERTATION

Presented to the Faculty of the Graduate School of the  
MISSOURI UNIVERSITY OF SCIENCE AND TECHNOLOGY

In Partial Fulfillment of the Requirements for the Degree

DOCTOR OF PHILOSOPHY

in

CHEMICAL ENGINEERING

2011

Approved

David B. Henthorn, Advisor  
Chang-Soo Kim, Co-advisor  
Douglas K. Ludlow, Co-advisor  
Yangchuan Xing  
Roger F. Brown

© 2011

Zhan Gao

All Rights Reserved

### **PUBLICATION DISSERTATION OPTION**

The dissertation consists of the following three articles that have been submitted for publication, or will be submitted for publication as follows:

Pages 17-32 was published on JOURNAL OF MICROMECHANICS AND MICROENGINEERING.

Pages 34-56 are intended for submission to IEEE SENSORS JOURNAL.

Pages 58-70 are intended for submission to SENSORS AND ACTUATORS B: CHEMICAL.

## ABSTRACT

The surface modification, fabrication and characterization of microfluidic sensor systems for oxygen and glucose measurements with the use of polymeric materials were investigated in this dissertation. This dissertation is prepared in publication format. The first manuscript focuses on the surface modification of SU-8 layer to enhance the wettability. The improvement of wettability is critical since biofouling can be minimized during bioanalysis. A novel *in situ* photopatternable grafting technology was used to attach biocompatible polymer layers on SU-8 surface, changing its property from hydrophobicity to hydrophilicity. The results were confirmed by contact angle measurement and Fourier Transform Infrared (FTIR) spectra. The second manuscript demonstrates the use of modified SU-8 for applications to microfluidic sensors for dissolved oxygen measurements based on quenching behavior of fluorophore. A new chemical anchoring method was introduced to lithographically pattern sensing elements inside a complete SU-8 microfluidic channel. A stable Stern-Volmer relationship between oxygen content and fluorescent intensity was observed for two months. The third manuscript is about the fabrication and characteristic of fluorescent glucose microfluidic sensor by using an optically transparent dry film, PerMX 3050. It was possible to determine the glucose concentrations by the normalized initial reaction rates, derived from the fluorescent intensity change caused by enzymatic oxygen consumption. Novel polymer materials and surface modification technologies introduced in this dissertation have been successfully applied to optical microfluidic sensors and exhibit a large potential for many other biomolecules assay.

## ACKNOWLEDGMENTS

I would like to take this opportunity to thank everybody who helped me finish my research over the past five years.

First, I would especially like to express my gratitude to my advisor, Dr. David B. Henthorn; I thank him for giving me the chance to work with him and for his invaluable advice, patience and encouragement.

I would like to thank my co-advisor, Dr. Chang-Soo Kim for his wise guidance and valuable comments to my research.

I am grateful to Dr. Douglas K. Ludlow, Dr. Yangchuan Xing, and Dr Roger F. Brown for being my committee members.

I wish to thank my parents, husband, and all my friends for their love, support and encouragement.

## TABLE OF CONTENTS

	Page
PUBLICATION DISSERTATION OPTION .....	iii
ABSTRACT .....	iv
ACKNOWLEDGMENTS .....	v
LIST OF ILLUSTRATIONS .....	x
LIST OF TABLES .....	ix
<b>SECTION</b>	
1. INTRODUCTION .....	1
1.1. OPTICAL OXYGEN SENSOR .....	1
1.1.1. Oxygen Quenching of Fluorophore.....	1
1.1.2. Ruthenium Complex.....	3
1.2. OPTICAL GLUCOSE SENSOR.....	3
1.2.1. Glucose Measurement Based on Enzyme Reaction.....	3
1.2.2. Glucose Oxidase (GOD) and Enzyme Activity .....	5
1.3. COMMON POLYMER MATERIALS FOR FLUIDIC CHANNEL .....	7
1.3.1. Poly (dimethylsiloxane) (PDMS).....	7
1.3.2. SU-8 Epoxy-Based Photoresist .....	7
1.3.3. Dry Film Photoresist (DFR).....	9
1.4. SURFACE MODIFICATION .....	10
1.4.1. Free Radical Polymerization .....	10
1.4.2. Photoinduced SU-8 Surface Modification .....	11
1.5. PEG-BASED HYDROGEL .....	13
REFERENCES .....	14
<b>PAPER</b>	
I. Enhanced wettability of an SU-8 photoresist through a photografting procedure for bioanalytical device applications .....	18
ABSTRACT.....	18
1. INTRODUCTION .....	18
2. MATERIALS AND METHODS.....	20

2.1. Materials .....	20
2.2. Preparation of SU-8 samples .....	20
2.3. Characterization of modified surface .....	21
2.4. Photografting .....	21
2.5. Micropatterning .....	22
3. DISCUSSIONS .....	23
3.1. Effect of hydrogel composition on wettability .....	23
3.2. Effect of polymerization time .....	24
3.3. PEG surface layer .....	25
3.4. Verification of proposed reaction .....	31
3.5. Photopatterning of PEGDMA .....	32
4. CONCLUSIONS .....	34
ACKNOWLEDGMENTS .....	34
REFERENCES .....	35
II. Sensor application of poly (ethylene glycol) diacrylate hydrogel chemically anchored on polymer surface .....	37
ABSTRACT .....	37
1. INTRODUCTION .....	37
2. EXPERIMENTAL .....	40
2.1. Materials .....	40
2.2. Surface immobilized oxygen-sensitive hydrogel membrane formation ...	40
2.2.1 Preparation of SU-8 films .....	40
2.2.2 Chemical anchoring procedure .....	41
2.2.3 SU-8 channel fabrication .....	42
2.3. Instrumentation .....	45
3. RESULTS AND DISCUSSIONS .....	46
3.1. Verification of chemical anchoring scheme .....	46
3.2. Effect of photoinitiation process and initial photostability .....	47
3.3. Spectral response and initial stability .....	48
3.4. Effect of ruthenium concentration on relative sensitivity .....	49
3.5. Response time and reversibility .....	53

3.6. Long-term storage stability .....	56
3.7. Dissolved oxygen measurements within SU-8 channel .....	58
4. CONCLUSIONS .....	60
ACKNOWLEDGMENTS .....	60
REFERENCES .....	61
III. A dry film fluorescence glucose microfluidic sensor with in-device PEG-based sensing element.....	63
ABSTRACT .....	63
1. INTRODUCTION .....	63
2. EXPERIMENTAL.....	65
2.1. Materials.....	65
2.2. Glucose oxidase (GOD) activation .....	66
2.3. Dry film channel fabrication .....	66
2.4. Integration of glucose sensing elements .....	69
2.5. Device design .....	70
2.6. Instrumentation .....	72
3. RESULTS AND DISCUSSIONS .....	72
3.1. Typical time response .....	73
3.2. Calibration curve for glucose measurement.....	75
3.3. The effect of GOD concentrations .....	77
3.4. Reversibility and repeatability .....	78
4. CONCLUSIONS .....	79
REFERENCES .....	80
SECTION	
APPENDICES	
A. DETAILED PROCEDURES FOR SU-8 CHANNEL FABRICATION AND OXYGEN SENSING ELEMENTS.....	82
B. DETAILED PROCEDURES FOR PerMX CHANNEL FABRICATION AND GLUCOSE SENSING ELEMENTS .....	85
VITA .....	88

## LIST OF ILLUSTRATIONS

Figure	Page
1.1. Underlying principle for enzyme-based optical glucose sensor.....	4
1.2. The functional modification of glucose oxidase by acryloyl chloride .....	5
1.3. Formula structure of SU-8 photoresist .....	9
1.4. Schematic diagram for the photoinduced graft polymerization of monomer onto a SU-8 surface .....	12
 PAPER I	
1. Schematic diagram for the photoinduced graft polymerization of monomer onto a SU-8 surface .....	22
2. Static water contact angle decreases with increasing percentage of HEMA in prepolymerization mixture .....	23
3. Influence of polymerization reaction time on surface wettability for 95% HEMA hydrogel on SU-8 .....	24
4. ATR-FTIR spectra: pHEMA photo-grafting on SU-8 surface.....	26
5. ATR-FTIR spectra: PEGDMA hydrogel on SU-8 surface .....	27
6. ATR-FTIR subtraction spectra: PEGDMA hydrogel on SU-8 surface .....	28
7. ATR-FTIR subtraction spectra: PEGDMA hydrogel on SU-8 surface.....	29
8. Scanning electron micrographs of PEGDMA (Mn=875) gel microstructures on SU-8 surface .....	33
 PAPER II	
1. Preparation of oxygen-sensitive hydrogel anchored on SU-8 surface. a) Ruthenium complex and PEG-DA monomers mixture filled out the space of glass cover/spacer/SU-8 assembly; b) PEG-DA membrane was chemically anchoring on the photoinitiated SU-8 surface after UV exposure. ....	42
2. Fabrication process scheme of optical fluidic dissolved oxygen sensor .....	44
3. Experimental setup with spectroscopic equipment and controlled gas composition for fluorescent oxygen detection .....	46
4. Initial stability of the fluorescent emission from ruthenium complex during 12 hours after incorporation in chemically anchored PEG-DA membranes on SU-8 surface.....	48
5. Optical properties of oxygen sensitive PEG-DA membranes on SU-8 surface .....	52
6. Response time and reversibility of fluorescence intensity changes of PEG-DA membrane upon switching between nitrogen and oxygen saturated D. I. water repeatedly (a) The sample stored in D.I. wafer for 1 day (b) The sample stored in D.I. water for 2 months .....	55

7. Long-term stability of ruthenium complex incorporated in chemically anchored PEG-DA membrane on SU-8 surface .....57
8. Dissolved oxygen measurements for cylindrical PEG-based sensing structure chemically anchored after bonding process .....59

### PAPER III

1. The functional modification of glucose oxidase by acryloyl chloride .....66
2. Bonding procedure of PerMX fluidic channel structure .....68
3. Cross-sectional diagram of PEG-based hydrogel with entrapped ruthenium complex and immobilized GOD .....69
4. Top view diagrams and photography of integrated fluorescent glucose microfluidic channel .....71
5. Measurement setup for optical glucose PerMX DFR fluidic channel sensor .....72
6. Typical response curves for glucose measurements .....74
7. Rate of initial intensity change rate as a function of glucose concentrations (PBS solution,  $\text{pH}=7.42 \pm 0.1$ , duration time =5 min). .....76
8. The effect of GOD concentrations on normalized initial rate (Series 1:  $[\text{GOD}]=0.012\text{mM}/\text{ml}$  PEGDA,  $n=9$ ; Series 2:  $[\text{GOD}]=0.033\text{mM}/\text{ml}$  PEGDA,  $n=9$ ; Series 3:  $[\text{GOD}]=0.056\text{mM}/\text{ml}$  PEGDA,  $n=6$ ). .....78

**LIST OF TABLES****PAPER I**

1. Contact angle measurement of PEG modified SU-8 surface ..... 30
2. Static water contact angle measurements of HEMA modified SU-8 for triple repeats in air and in oxygen free environments to verify surface initiator role..... 31

**PAPER II**

1. Fluorescence intensity before and after UV polymerization..... 48

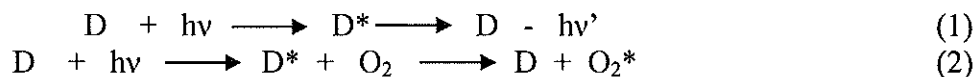
## 1. INTRODUCTION

Microfluidic devices, fabricated with micromechanic technology, can be identified by the fact that it has one or more channels with at least one dimension less than 1 mm. The origin of modern microfluidics can be traced back to the research about a gas chromatograph on a silicon chip at Stanford University and ink jet printer nozzles by IBM in the late 1970s. Though the development of those two devices was groundbreaking, microfluidics had not developed into a hot research area until the concept of micrototal analysis systems or Lab-on-a-chip was adapted in the early 1990s. The most significant advantage of these Lab-on-a-chip devices (or micrototal analysis systems) was to miniaturize the size of sensing system, being accompanied by reduced reagent consumption, increased automation, and reduced manufacturing costs [1].

Traditionally, microfluidic devices are mostly fabricated with silicon, if transparent setups are necessary, with glass. Silicon- and glass- based microfluidic channel fabrication requires complex, time-consuming and expensive process. In recent years, polymers have become popular materials in channel fabrication because of the ease and low cost of manufacturing. These polymers include poly (methylmethacrylate) (PMMA), polyvinylchloride (PVC), poly (dimethylsiloxane) (PDMS) and Photoresist. Among these materials, PDMS and photoresist (e.g. SU-8, dry film) have attracted more attention due to their special properties described as bellow.

### 1.1. OPTICAL OXYGEN SENSOR

**1.1.1. Oxygen Quenching of Fluorophore.** A common approach to design fluorescent oxygen sensor involves transduction of the changes in luminescence characteristics of both organic and inorganic dyes immobilized in different matrixes. In general, the underlying principle of most fluorescent oxygen sensors is the quenching behavior of the dye's fluorescence towards oxygen molecules. This principle was first introduced by Kautky and Hirsch during 1930's [2, 3] and applied to fabricate the first complete optical oxygen sensor system in 1968 by Bergman [4]. The details of this underlying principle are described in Eq. (1) and Eq. (2) [5].



Where, D (D\*) is fluorescence dye at ground state (excited state); O<sub>2</sub> (O<sub>2</sub>\*) is indicator molecules at ground state (excited state); hv is the energy generated by the light source with excitation wavelength of 470 nm; and hv' is the energy generated by the light source with emission wavelength of ~610 nm.

In this simple scheme, the fluorescence process in absence of oxygen molecules is described by Eq. 1 while the deactivation process of the dyes at excited state in presence of oxygen molecules is described by Eq. (2). During the deactivation process of the dyes at excited state, the energy is transferred from D\* to oxygen molecules after the collisions between them. Consequently, the measurable fluorescence signal decreases with the presence of oxygen molecules. The collision between the dye and the indicator (oxygen molecules), which leads to the less fluorescent signal emission is called collisional or dynamic quenching.

The oxygen detection by luminescence quenching can be described by the Stern-Volmer equation [6], which was first discovered by Otto Stern and Max Volmer in 1919, in a homogeneous medium, such as an aqueous solution. The Stern-Volmer equation is demonstrated as follows:

$$\frac{I_0}{I} = \frac{\tau_0}{\tau} = \frac{\Phi_0}{\Phi} = 1 + K_{SV}[O_2] \quad (3)$$

$$K_{SV} = k\tau_0 \quad (4)$$

where I<sub>0</sub> (τ<sub>0</sub>, Φ<sub>0</sub>), and I (τ, Φ) are the fluorescent intensities (the fluorescent lifetime, the phase shift of fluorophores) in the absence and presence of the dissolved oxygen molecules; [O<sub>2</sub>] is defined as percent oxygen saturation (i.e. a sample of 50% percent oxygen saturation refers to D.I. water that has been saturated with a gas comprised of 50% oxygen and 50% nitrogen by mole at atmosphere pressure) in this work. K<sub>sv</sub> is the Stern-Volmer quenching constant, while k is the quencher rate coefficient. Under isothermal and isobaric conditions, K<sub>sv</sub> should remain constant, and the relationship between relative sensitivity I<sub>0</sub>/I and [O<sub>2</sub>] is linear. In most work on optical oxygen sensors, in

order to protect the fluorescence dyes from the interaction with other species in testing solution, dyes are immobilized in the oxygen permeable matrixes, such as silicone rubber, polymethyl methacrylate (PMMA) and polyvinyl chloride (PVC) [5]. It has been observed that, in contrast to homogeneous solutions, the Stern-Volmer plot of  $I_0 / I$  versus saturation oxygen concentration deviates from linear relationship when oxygen level is high. This is a common feature of ruthenium complex physically immobilized in matrix and can be explained by two models [7-9]. The details about this phenomenon and the two models are described in the second manuscript in Section.3.

**1.1.2. Ruthenium Complex.** Organometallic compounds are usually used as fluorescence dyes in optical oxygen sensors since they have special properties, such as strong luminescence with long lifetime and large stocks-shift. There are various kinds of organometallic compounds including polycyclic aromatic hydrocarbons (pyrene, pyrenederivative etc.), transition metal complexes ( $Ru^{2+}$ ,  $Os^{2+}$ ,  $Ir^{2+}$ , etc.), and metalloporphyrins ( $Pt^{2+}$ ,  $Pd^{2+}$ ,  $Zn^{2+}$ , etc.) [10]. Among these fluorescence dyes, Ruthenium complex has been investigated extensively due to its reversible quenching behavior toward oxygen molecules, long-term photostability, and strong fluorescent signals [9]. In our work, the emission wavelength and excitation wavelength of ruthenium complex are 470 nm and 608 nm respectively.

## 1.2. OPTICAL GLUCOSE SENSOR

**1.2.1. Glucose Measurement Based on Enzyme Reaction.** Diabetes ranks the sixth leading cause of death in the world and 10.3 million elder people are now suffering from it in United States. The diagnosis and management of diabetes mellitus require a continuous monitoring of blood glucose level. The initial concept of glucose enzyme sensor was proposed by Clark and Lyons [11]. Their first device was constructed with an oxygen electrode covered by a thin layer of glucose oxidase (GOD) entrapped in a semipermeable dialysis membrane to detect the oxygen consumption during the glucose oxidase enzyme reaction (as shown in Eq. 5). It is hard for this first generation electrochemical oxygen sensor to obtain accurate oxygen measurement, since the background  $O_2$  concentration in biological fluid or in ambient environment fluctuates frequently. In order to distinguish the signal caused by the background fluctuation from

that generated by the oxygen consumption, a secondary counter-oxygen electrode without immobilized glucose oxidase was added by Updike and Hicks [12]. However, the glucose measurement at the low oxygen level was still not accurate due to the consumptions of oxygen by the electrodes [13]. Figure 1.1 describes underlying principle for enzyme-based optical glucose sensor.

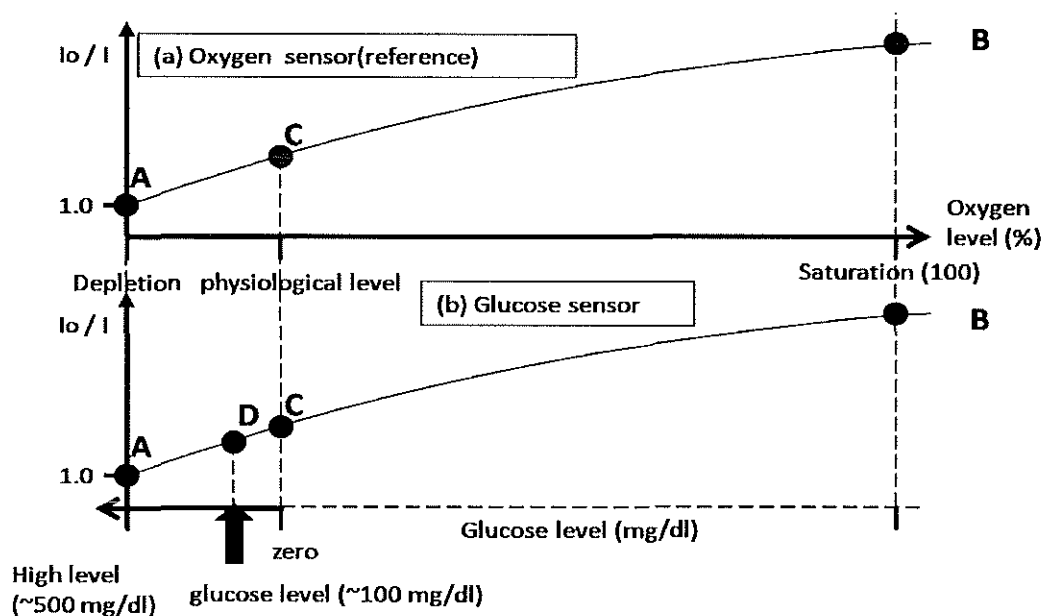


Figure 1.1. Underlying principle for enzyme-based optical glucose sensor.



Enzyme-based glucose sensors with fluorescence transducer are receiving increasing attention these days since all the problems mentioned above can be solved. Generally, fluorescent enzyme-based sensors are designed by using specific fluorescent dyes to either detect the depletion of oxygen molecules or measure the generation of the

hydrogen peroxide. In our work, the enzyme-based fluorescence glucose sensor based on the oxygen consumption during GOD reaction is studied. The underlying principle of this optical glucose sensor is depicted in Figure 1.1. In this figure, oxygen content is considered to be at physiological level in absence of glucose molecules. With the increase of glucose level from point C to point A, the relative intensity of sensor ( $I_0 / I$ ) decreases gradually. It is understandable since the fluorescent intensity ( $I$ ) goes up with the consumption of oxygen molecules. Based on change of fluorescent intensity, glucose concentrations can be detected.

**1.2.2. Glucose Oxidase (GOD) and Enzyme Activity.** GOD is one of the most widely used enzymes for the enzyme-based biosensor fabrication due to its relatively low cost and commercial availability with high purity. It was first discovered by Müller in *Aspergillus niger* and *Penicillium glaucum* and found to oxidize the glucose to gluconic acid in the presence of oxygen molecules. Considering recovery of the enzyme for repetitive use, GOD enzymes are normally immobilized in membranes, serving as sensing elements in biosensor [14]. In our project, GOD is modified by acryloyl chloride and chemically immobilized in PEG membrane (as shown in Figure 1.2.) with the similar recipe from the method reported by Dr. Peppas' group [15].

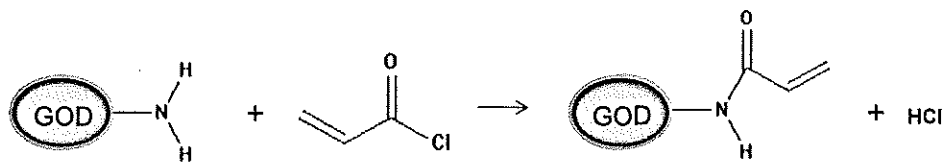


Figure 1.2. The functional modification of glucose oxidase by acryloyl chloride.

The kinetics and mechanisms of GOD enzyme reaction is an efficient tool to be used to design the optical glucose microfluidic sensor and optimize the parameters in the future work. Michaelis and Menten rate equation is often adopted to analyze the performance of enzyme-based sensor and is conveniently written as follows:

$$v = \frac{V_1(\text{max.})[S]}{K_m + [S]} \quad (6)$$

Michaelis and Menten formulated this rate equation for one-substrate reactions having a signal intermediate. However, this equation is not applicable for two-substrate reaction since glucose is not the only substrate in this reaction.

For this two-substrate reaction, a general form of equation is displayed as follow [5]:

$$v = \frac{V_1[A] \cdot [B]}{K'_A K_B + K_B[A] + K_A[B] + [A] \cdot [B]} \quad (7)$$

Where [B] is glucose concentration, [A] is oxygen concentration.  $K'_A$ ,  $K_B$ ,  $K_A$ ,  $V_1$  are four kinetic parameters.

Equation (7) in the Michaelis form is:

$$v = \frac{V_1(\text{max.})[B]}{K_A(\text{app.}) + [B]} \quad (8)$$

Here, for any value of [B], the apparent Michaelis constant for [A] is

$$V_1(\text{max.}) = \frac{V_1[A]}{K_A + [A]} \quad (9)$$

For any value of [B], the maximum reaction rate for [A] is

$$K_A(\text{app.}) = \frac{K'_A K_B + K_B[A]}{K_A + [A]} \quad (10)$$

At the very beginning of enzyme oxidation reaction, oxygen concentration is considered to be constant. In this case,  $V_1(\text{max.})$  and  $K_A(\text{app.})$  are both constants. Thus,

at this moment, Michaelis equation for single substrate can be adopted to describe the two-substrate enzyme reaction.

### 1.3. COMMON POLYMER MATERIALS FOR FLUIDIC CHANNEL

**1.3.1. Poly (dimethylsiloxane) (PDMS).** PDMS is the most widely used organic polymer for optical biosensor fabrication and commonly referred to as silicones. Normally, PDMS is used to construct the microfluidic channel through soft lithography, a technology first introduced by Whiteside's group [16]. According to this technology, PDMS microfluidic structure can be achieved by pulling polymerized PDMS off from the designed micromold. No damage will be left either to PDMS microfluidic structure or to the micromold due to its elasticity property. Many other properties, such as optical clarity, biological inertness also make PDMS an attractive material for the fabrication of optical sensor, especially used in biological area [17].

However, some properties as follows prevent PDMS from being a good structure material for the optical GOD-based sensor.

- 1) PDMS is permeable to oxygen molecules in ambient air [18]. Although this property is good for the fabrication of biosensor used for cell cultures, which requires continuous supply of oxygen, it is a negative effect on the fluorescent intensity measurement based on the oxygen quenching behavior.
- 2) PDMS is extremely hydrophobic [19], which leads to the biofouling and nonspecific adsorption of enzyme if human blood was used as the sample solution. In this project, the purpose of our optical glucose sensor is to detect the glucose level in human blood. Thus, whether the biofouling can be minimized or not is very critical.
- 3) Soft lithography technique is not compatible with traditional lithography process, which makes it difficult to obtain PDMS chips in industry.

**1.3.2. SU-8 Epoxy-based Photoresist.** Photoresist, photosensitive materials used in the microelectronics industry, have been investigated extensively and represent an attractive alternative to PDMS for optical oxygen (glucose) sensor fabrication. SU-8 is a negative-tone epoxy-based photoresist that was first introduced and patented by IBM in 1989 [20]. The resist consists of an EPON SU-8 resin and a photoacid generator, triaryl

sulfonium salts. SU-8 photoresist is found to be particularly well suitable as channel structure since a wide range of structure thickness (from 2 to 300  $\mu\text{m}$ ) can be achieved through traditional lithography system. Compared with PDMS microfluidic channel, sealed SU-8 microfluidic channel is a better candidate to be integrated with oxygen-sensitive sensing elements for the following reasons:

- 1) SU-8 is less oxygen permeable to oxygen molecules. Different from PDMS, SU-8 is one kind of glassy polymers. In general, the oxygen diffusion coefficient is low for most of glassy polymers [18].
- 2) SU-8 has a high functionality. The epoxy groups of SU-8 photoresist make many surface modification methods possible to carry out (SU-8 formula is shown in Figure 1.3).
- 3) Compared with the traditionally bonding process, simple equipments are required for SU-8 channel bonding by using adhesive bonding method. At the early stage of adhesive bonding method for SU-8 channel bonding, crosslinked SU-8 was used as a bonding layer. Although successful bonding could be achieved, the whole process should take place in vacuum environment under high temperature using dedicated equipments [21]. Typical pressure, temperature, and bonding time are 3 bars, 100  $^{\circ}\text{C}$ , and 20 min respectively [22]. For adhesive bonding method with uncross-linked SU-8 itself as glue [23], only an UV aligner and a hotplate are required.

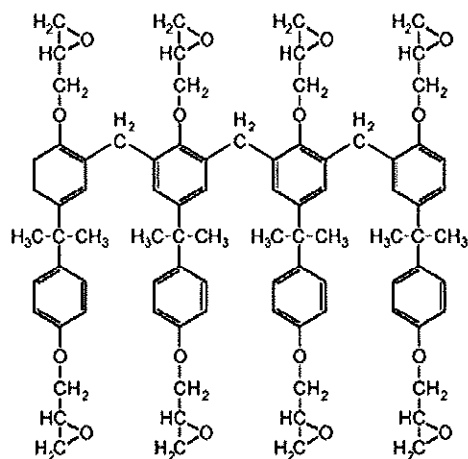


Figure 1.3. Formula structure of SU-8 photoresist [24]

**1.3.3. Dry Film Photoresist (DFR).** During the past decades, the majority of polymeric microfluidic devices are created using PDMS since it can be easily processed by molding and commercially available at low cost [18]. A significant disadvantage of these PDMS microfluidic channels is that with standard process only one substrate, typically the bottom substrate, can be modified to integrate with sensing elements. With the increase of the complexity of microfluidic devices, however, monolithic channels sometimes are required to ensure the uniform surface property inside. In order to come to such a monolithic channel structure, negative-tone, epoxy-based SU-8 photoresist was utilized as a popular structure material since 1990s [20]. Unlike PDMS, SU-8 channel structures can be created with a single photolithography step. In addition, adhesive bonding method, an inexpensive bonding technology especially suitable for SU-8 channels have been reported to enable successful channel bonding at low temperature with a high surface roughness tolerance. However, the maximum SU-8 channel thickness is limited because inhomogeneous deposition on substrate caused by spin-coating process. The bond yield is reported to decrease dramatically from 95% to 55% at a thickness

deviation of 1.3%, resulting in higher change of failure for monolithic channel fabrications [25].

Generally, compared with SU-8 photoresist, DFRs yields layers with a low thickness deviation since they are normally applied through lamination. They have been reported useful for fabricating hybrid microfluidic channels, because they obtain special properties, such as good adhesion to glass substrate, good flatness, and no formation of edge beads, short processing time and near vertical sidewall [26]. In addition, the setting up cost is relatively low and fabrication steps are not as complicated as liquid photoresist. So far, established DFRs for microfluidic channel fabrication are Ordyl series from Elga Eurpe Company. Although this DFR demonstrates applicable for creating microfluidic structures in many publications [25, 26], the applications in monolithic channel integrated with optical sensing elements is restricted due to its optical mistiness. Recently, novel transparent DFRs, PerMX 3000 series [27], were available from DuPont Company and utilized as structure material for channel fabrication in our project.

#### 1.4. SURFACE MODIFICATION

**1.4.1. Free Radical Polymerization.** Free radical polymerization is any polymerization involving free radicals. This concept was first introduced at the turn of the 20th century and attracted the interest of the scientists in middle of 1930s. In general, free radiation polymerization consists of three steps: initiation, chain propagation and chain termination (As shown from Eq. 11 to Eq. 16). Normally, the initiation takes place by cleavage of azos or peroxide compounds to yield the “primary radicals”. These primary radicals are called initiators. These initiators are bound to polymer substrate through the hydrogen abstract reaction [28] to form the initiated substrate. Under the UV irradiation in the propagation step, the monomer will take the place of the primary radical on the surface or of the radical at the end of the growing polymer chain. Finally, the propagation reaction will be terminated by the reaction of two growing polymer with radicals.

Initiation:



Propagation:



Termination:



Nowadays, free radical polymerization is widely used for the synthesis of long chain polymer with functional groups like methacrylate, styrene, acrylonitrile and ethylene. In our work, this technique is adapted to change SU-8 surface properties or chemically anchor the sensitive membrane. This process will slow down if the inhibitors, oxygen molecules, are present [29]. In order to eliminate the inference with the oxygen molecules, all the free radical polymerization should be taken place at a nitrogen atmosphere.

**1.4.2. Photoinduced SU-8 Surface Modification.** Although SU-8 is considered a good candidate as structure material for microfluidic channel, hydrophobic property of SU-8 surface is an issue. It will make the testing solution difficult to flow through the microfluidic channel and result in “bio-fouling” (deposition and growth of microorganisms on surface). Thus, wettability of SU-8 surface becomes very critical.

In order to achieve the hydrophilic surface inside SU-8 microfluidic, surface modification technique should be applied. This technique possesses two unique advantages: (1) to change the surface properties of SU-8 photoresist without affecting its bulk property; (2) to eliminate the need of the channel structure redesign or the change of polymer structure materials to achieve the target surface performance. Common ways to modify SU-8 are to react with oxygen plasma [30] or to graft hydrophilic polymer by utilizing cerium (IV) ammonium nitrate (CAN) [31] or to be treated with sulfuric acid [32]. Although these approaches do enhance the wettability of SU-8 surface, they also suffer from some weaknesses. The modification effect caused by oxygen plasma would remain only for a short period while the modification process through CAN and sulfuric acid requires a long and complicated treatment steps. In our work, photoinduced grafting technique by UV irradiation is introduced to change the property of SU-8 surface from

hydrophobicity to hydrophilicity. The underlying principle was displayed in Figure 1.4. Fast reaction rate, low cost of processing, simple equipment and easy industrialization are all considered as the advantages of this technique.

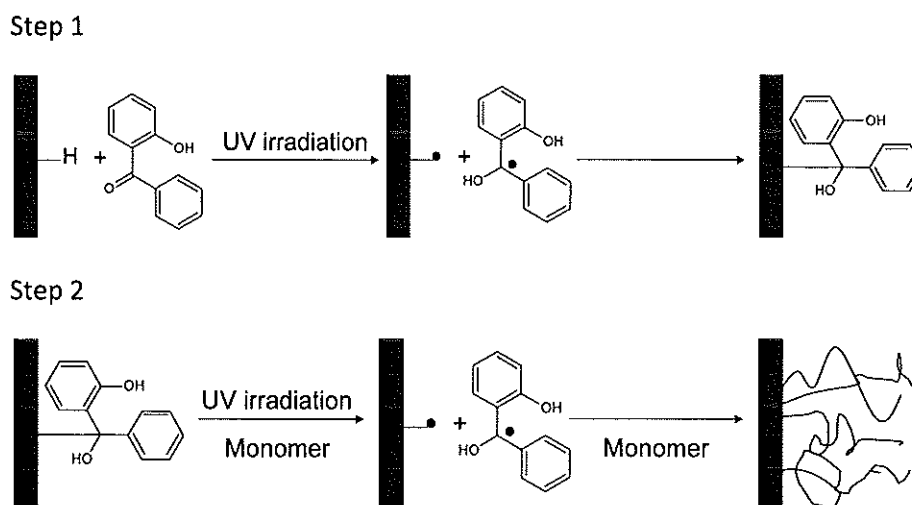


Figure 1.4. Schematic diagram for the photoinduced graft polymerization of monomer onto a SU-8 surface.

The pioneering work on photografting polymerization initiated by UV light was published in the 1950s by Oster and Shibata [33]. In the last decade, since the SU-8 photoresist became the main stream structure materials to fabricate microfluidic channel for biological applications, different strategies of surface modification of SU-8 by this technique have been developed rapidly and numerous papers have been published. Wang et al. reported two methods for the photografting of poly (ethylene glycol) (PEG) from the surface of SU-8 photoresist [31, 34]. In the first method, PEG chains were grafted from the SU-8 surface through a free radical reaction using the photoacid generator triarylsulfonium hexafluoroantimonate as a photoinitiator [34]. In the second method, surface exposed epoxy groups of SU-8 photoresist were chemically converted into hydroxyl groups, which then served as initiation sites for the graft polymerization of PEG on SU-8. Both of the methods were catalyzed by cerium (IV) ammonium nitrate in the acid environment [31]. Desai et al [35] also conducted a lot of research on SU-8 surface

modification. In their work, aminopropyltriethoxysilane was used as a bridge to couple the PEG monomers to SU-8 surface, whose epoxy groups were opened by using concentrated sulfuric acid [35]. In our work, a 'graft from' technique, derived from work done by Ma et al [36] was used to produce grafted polymer layers on the SU-8 layer. HCPK, as photoinitiator and PEG, as grafted material, were adapted in this method. The details about the underlying principle of this method are shown in Figure 1.4. and will be described in the later section.

### 1.5 PEG-BASED HYDROGEL

Photopatternable PEG-based hydrogel matrix used to physically entrap the fluorescent dye or covalently immobilize the enzyme has recently received a lot of attention in the application of bio-micro-electro-mechanical system. This kind of matrix is a good candidate for optical biological sensors for several reasons as follows [37]:

- 1) PEG-based hydrogel is biocompatible. Since the optical glucose sensor is designed to test the blood glucose level, it is very important to eliminate the biofouling caused by the nonspecific adsorption of microorganism.
- 2) PEG-based hydrogel exhibits the ability to swell in the water and retain a significant fraction of water within its structure without dissolving. Thus these small hydrophilic molecules, especially the analyte, can diffuse into the hydrogel easily and contact with fluorescent dyes or enzymes.
- 3) PEG-based hydrogel is transparent, which makes the optical detection possible.

Many methods about PEG-based hydrogel used as matrix for different fluorescent dyes or various biomolecules are reported recently [37, 38]. However, most of the PEG-based hydrogels are polymerized inside the microfluidic channel before SU-8 bonding process. These biomolecules (such as enzyme, antibody, and etc.) are going to lose their activity since high temperature is required for normal bonding process. In our work, this photoinduced technique is used to chemically anchor the PEG-based hydrogel on the SU-8 surface within sealed fluidic channel. The details about physical entrapment of ruthenium complex and chemical immobilization of GOD with PEG-based hydrogel are described in later sections.

## REFERENCES

- [1] P. Gravesen, J. Branebjerg, O. S. Jensen, "Microfluidics-a review," *J. Micromech. Microeng.* 3, 168-182, 1993.
- [2] H. Kautsky and A. Hirsch, "Interactions of excited dye molecules and oxygen," *Ber. Deut. Chem. Ges*, 64, 2677, 1931.
- [3] H. Kautsky, "Quenching of luminescence by oxygen," *Trans. Faraday Soc.*, 35, 216-219, 1939.
- [4] I. Bergman, "Rapid- response atmospheric oxygen monitor based on fluorescence quenching," *Nature*, 218, 396, 1968.
- [5] R. Ramanoorthy, P. K. Dutta, S. A. Akbar, "Oxygen sensors: materials, methods, designs and applications" *Chem. Sens.*, 38, 4271-4282, 2003.
- [6] A. Mills, Optical oxygen sensors: utilizing the luminescence of platinum metals complexes, *Platinum Met. Rev.*, 41, 115-127, 1997.
- [7] E. R. Carraway, J. N. Demas, B. A. DeGraff, "Luminescence quenching mechanism for microheterogeneous systems," *Anal. Chem.*, 63, 332-336, 1991.
- [8] E. R. Carraway, J. N. Demas, B. A. DeGraff, J. R. Bacon, "Photophysics and photochemistry of oxygen sensors based on luminescent transition-metal complexes," *Anal. Chem.*, 63, 337-342, 1991.
- [9] J. N. Demas, B. A. DeGraff, W. Y. Xu, "Modeling of luminescence quenching-based sensors: comparison of multisite and nonlinear gas solubility models," *Anal. Chem.*, 67, 1377-1380, 1995.
- [10] Y. Amao, "Probes and polymers for optical sensing of oxygen," *Microchim. Acta.*, 143, 1-12, 2003.
- [11] J. Wang, "Electrochemical glucose biosensor," *Chem. Rev.*, 108, 814-825, 2008.
- [12] S. J. Updike, G. P. Hicks, "The enzyme electrode," *Nature*, 214, 986-988, 1967.
- [13] D.P. O' Neal, M.A. Meledeo, J.R. Davis, B.L. Ibey, V.A. Gant, M.V. Pishko, G.L. Coté, Oxygen sensor based on the fluorescence quenching of a ruthenium complex immobilized in a biocompatible poly(ethylene glycol) hydrogel, *IEEE Sens. J.*, 4, 728-734, 2004.
- [14] J. Raba, H. A. Mottola, "Glucose oxidase as an analytical reagent," *Cr. Rev. Anal. Chem.*, 25(1), 1-42, 1995.

- [15] C. M. Hassan, F. J. Doyle III, N. A. Peppas, "Dynamic behavior of glucose-responsive poly(methacrylic acid-g-ethylene glycol) hydrogels," *Macromolecules*, 30, 6166-6173, 1997.
- [16] Y. Xia, G. M. Whitesides, "Soft lithography," In *Prog. Chem. Int. Ed. Engl.* 37, 551-575, 1998.
- [17] W-G Koh, M. Pishko, "Photoreaction injection molding of biomaterial microstructures," *Langmuir*, 19, 10310-10316, 2003.
- [18] H. X. Rao, F. N. Liu, Z. Y. Zhang, "Preparation and oxygen/nitrogen permeability of PDMS crosslinked membrane and PDMS/tetraethoxysilicone hybrid membrane," *J. Membrane Sci.*, 303, 132-139, 2007.
- [19] H. Makamba, J. H. Kim, K. Lim, N. Park, J. H. Hahn, "Surface modification of poly (dimethylsiloxane) microchannels," *Electrophoresis*, 24, 3607-3619, 2003.
- [20] H. Lorenz, M. Despont, N. Fahrni, N. LaBianca, P. Renaud, P. Vettiger, "SU-8: a low-cost negative resist for MEMS," *J. Micromech. Microeng.*, 7, 121-124, 1997.
- [21] C. T. Pan, H. Yang, S. C. Shen, M. C. Chou, H. P. Chou, "A low-temperature wafer bonding technique using paterable materials," *J. Micromech. Microeng.*, 12, 611-615, 2002.
- [22] M. Agirregabiria, F. J. Blanco, J. Berganzo, M. T. Arroyo, A. Fullaondo, K. Mayoraa and J. M. Ruano-Lo'peza, "Fabrication of SU-8 multilayer microstructures based on successive CMOS compatible adhesive bonding and releasing steps," *Lab on a chip*, 5, 545-552, 2005.
- [23] R. J. Jackman, T. M. Floyd, R. Ghodssi, M. A. Schmidt, K. F. Jensen, "Microfluidic systems with on-line UV detection fabricated in photodefinable epoxy," *J. Micromech. Microeng.*, 11, 263-269, 2001.
- [24] N. C. Labianca, J. D. Gelorme, "High-aspect-ratio resist for thick-film applications," *Proc. SPIE*, 2438, 846-852, 1995.
- [25] T. Huesgen, G. Lenk, B. Albrecht, P. Vulto, T. Lemke, P. Woias, "Optimization and characterization of water-level adhesive bonding with patterned dry-film photoresist for 3D MEMS integration," *Sens. Actuators. A*, 162, 137-144, 2010.
- [26] P. Vulto, N. Glade, L. Altomare, J. Bablet, L. D. Tin, G. Medoro, I. Chartier, N. Maresi, M. Tartagni and R. Guerrieri, "Microfluidic channel fabrication in dry film resist for production and prototyping of hybrid chips," *Lab on a chip*, 5, 158-162, 2005.

- [27] K. Zhao, C. H. Wang, "Characterization of a photosensitive dry adhesive film for wafer level MEMS packaging" 2009 International conference on electronic packaging technology and high density packaging, August 10-13, 2009, Beijing, China.
- [28] N. A. Peppas, "Hydrogel in medicine and pharmacy," CRC press, Boca Raton, Florida.
- [29] W. Lee, D. Choi, J-H Kim, "Suspension arrays of hydrogel microparticles prepared by photopatterning for multiplexed protein-based bioassays," *Biomed Microdevices*, 10, 813-822, 2008.
- [30] C. K. Chung, Y. Z. Hong, "Surface modification of SU-8 photoresist for shrinkage improvement in a monolithic MEMS microstructure," *J. Micromech. Microeng.*, 17, 207-212, 2007.
- [31] Y. L. Wang, J- H Pai, H-H, Lai, C. E. Sims, M. Bachman, G. P. Li, N. L Allbritton, "Surface graft polymerization of SU-8 for bio-MEMS applications," *J. Micromech. Microeng.*, 17, 1371-1380, 2007.
- [32] S. L. Tao, K. Papat, T. A. Desai, "Off-wafer fabrication and surface modification of asymmetric 3D SU-8 microparticles," *Nat. protoc.*, 6, 3153-3158, 2006.
- [33] G. Oster, O. Shibata, "Graft copolymer of polyacrlamide and natural rubber produced by means of ultraviolet light," *J. Polym. Sci.*, 26, 233-234, 1957.
- [34] Y. L. Wang, M. Bachman, C.E. Sims, G.P. Li, N.L. Allbritton, "Simple photografting method to chemically modify and micropattern the surface of SU-8 photoresist," *Langmuir*, 22, 2719-2725, 2006.
- [35] S. L. Tao, K.C. Papat, J. J. Norman, T. A. Desai, "Surface modification of SU-8 for enhanced biofunctionality and nonfouling properties," *Langmuir*, 24, 2631-2636, 2008.
- [36] Walther F, Davydovskaya P, Zurcher S, Kaiser M, Herberg H, Gigler A M and Stark R W, "Stability of the hydrophilic behavior of oxygen plasma activated SU-8," *J. Micromech. Microeng.*, 17, 524-31, 2007.
- [37] Ma H, Davis and R H, Bowman C N, "A novel sequential photoinduced living graft polymerization," *Macromolecules*, 33, 331-5, 2000.
- [38] D. Choi, W. Lee, J. Park, W. Koh, "Preparation of poly(ethylene glycol) hydrogels with different network structures for the application of enzyme immobilization," *Biomed. Mater. Eng.*, 18, 345-356, 2008.

- [39] C. M. Hassan, F. J. Doyle III, N. A. Peppas, "Dynamic behavior of glucose responsive poly (methacrylic acid-g-ethylene glycol) hydrogels," *Macromolecules*, 30, 6166-6173, 1997.

## PAPER

### **I. Enhanced wettability of an SU-8 photoresist through a photografting procedure for bioanalytical device applications**

#### **ABSTRACT**

In this work, we detail a method whereby a polymeric hydrogel layer is grafted to the negative tone photoresist SU-8 in order to improve its wettability. A photoinitiator is first immobilized on freshly prepared SU-8 samples, acting as the starting point for various surface modifications strategies. Grafting of a 2-hydroxyethylmethacrylate-based hydrogel from the SU-8 surface resulted in the reduction of the static contact angle of a water droplet from  $79 \pm 1^\circ$  to  $36 \pm 1^\circ$ , while addition of a poly(ethylene glycol)-rich hydrogel layer resulted in further improvement ( $8 \pm 1^\circ$ ). Wettability is greatly enhanced after 30 minutes of polymerization, with a continued but more gradual decrease in contact angle up to approximately 50 minutes. Hydrogel formation is triggered by exposure to UV irradiation, allowing for the formation of photopatterned structures using existing photolithographic techniques.

#### **1. INTRODUCTION**

Most often, BioMEMS devices or biofluidic chips are fabricated from either glass- or silicon-based materials such as those used in traditional semiconductor or ceramic manufacturing. Various processes have been developed to create on-chip structures enabling these materials to be used as microdevices [1], but their broad use in bioanalytical microdevices has been limited by the difficult processing steps associated with fabrication. Strong chemical etchants, for example, are needed to produce such basic fluidic features as channels. Furthermore, the wafer bonding processes to seal fluidic channels require harsh conditions such as high temperature and/or high voltage, which make integration with biomolecules (enzymes, antibodies, etc.) challenging. As a

result, there has been growing interest in using organic-based, negative tone photoresists, such as the epoxy derived material, SU-8, in biofluidics applications [2]. Such photoresists allow for easy formation of high aspect ratio features with a simple expose-bake-develop procedure, even resulting in sealed channel structures formed under moderately low temperature [3]. However, for use in such applications it is of interest to improve the wettability of SU-8.

To date, researchers have focused on various methods to improve the aqueous wettability of SU-8. Measurements in our laboratory show that a freshly prepared SU-8 surface is not highly hydrophilic, with a static water contact angle of  $79 \pm 1^\circ$ . In order to improve the hydrophilicity of SU-8, a number of strategies have been employed by various researchers, including modification of the SU-8 bulk chemistry [4], the catalyzed addition of ethanolamine to the material surface [5], the use of ceric ammonium nitrate to graft poly(ethylene glycol) [6], and reaction with oxygen plasma [7,8]. In this work we demonstrate a novel method for the modification of SU-8 that seeks to provide the following features a.) improved wettability, b.) absence of harsh processing conditions such as high temperatures or strong chemical agents, c.) ability to integrate bioanalytical functional layers (e.g. enzyme immobilized hydrogels) within a completed fluidic channel, and d.) spatial control of such layers using traditional photolithographic techniques. Another disadvantage of traditional structure materials for microfluidic channels is nonspecific adsorption of reagent/sample molecules from the surrounding fluid-human blood (so called “biofouling”). While biocompatibility of SU-8 has been previously evaluated [9], our work aims to further decrease biofouling through addition of grafted polymer layers which are known to be biocompatible. Poly(ethylene glycol) (PEG), one of most widely used biocompatible polymer, was chosen to modify the SU-8 surface. It has been shown that PEG modified surfaces, including those in nanochannels, gain the ability to minimize nonspecific protein adsorption and cell attachment [10-12].

In this work, a “graft from” technique – photoinitiator is first immobilized on the material surface in a method derived from work done by Ma et al. [13] —is used to produce thin polymer layers on the substrate (SU-8) layer. Once modified, the now photoreactive surface may be brought in contact with various monomers. Irradiation with UV light begins a free radical polymerization that originates from the surface and

penetrates into the monomer liquid, resulting in covalent bound polymer chains. When this polymerization is done using hydrophilic monomers and crosslinker, the resulting grafted layer is a hydrogel – a material known for its wettability as well as its biocompatibility [14]. In this work we created grafted hydrogel layers composed of either 2-hydroxyethylmethacrylate (HEMA) monomer or of poly(ethylene glycol) (PEG) macromonomers. Polymeric HEMA (pHEMA) is known for its biocompatibility [14] and as such is found as the base material in soft contact lenses. Because of this, the transport of water and oxygen through pHEMA hydrogels has been studied [15] and it has subsequently attracted attention as a matrix for use in enzyme immobilization strategies [15, 16]. PEG is a well studied polymer frequently used to improve its biocompatibility and wetting properties of various materials [17].

## **2. MATERIALS AND METHODS**

### **2.1 Materials**

The photoinitiator 1-hydroxycyclohexyl phenyl ketone (HCPK), HEMA monomer, and tetraethyleneglycol dimethacrylate (TEGDMA) crosslinker were purchased from Sigma Aldrich (St. Louis, MO). PEG-rich hydrogels were formed using macromonomers of poly(ethylene glycol). Poly(ethylene glycol) monomethyl ether methacrylate (PEGMA) and poly(ethylene glycol) dimethacrylate (PEGDMA) were purchased from Sigma Aldrich. The macromonomers featured short PEG chains of  $M_n = 475$  and  $M_n = 875$  respectively. HEMA monomer was vacuum distilled prior to use in order to remove the free radical inhibitor hydroquinone monomethyl ether. Silicon wafers were purchased from University Wafer (South Boston, MA) and the negative tone photoresist SU-8 (formulation 2050) and propylene glycol methyl ether acetate were purchased from MicroChem (Newton, MA).

### **2.2 Preparation of SU-8 samples**

An SU-8 layer was added to the silicon wafers by spin coating at 2000 rpm for 15 seconds, followed by 3000 rpm for 38 seconds. A prebaking step included 4 minutes at 65 °C followed by a ramp to 95 °C for 8 minutes on a hotplate. The SU-8 initiator was activated by flood exposure to UV light in a mask aligner for 38 seconds for a total

exposure of 209 mJ/cm<sup>2</sup>. Post irradiation, the samples were then baked at 65 °C for one minute and then ramped to 95°C for nine minutes. Finally, the samples were developed with propylene glycol methyl ether acetate for 8 minutes and then rinsed with isopropanol followed by deionized water. This silicon wafer was cut into 1.5×1.5 cm small pieces, each of them with 1×1 cm SU-8 patterned layer. Those small pieces were soaked in ethanol for 12 hours and dried to constant weight.

### 2.3 Characterization of modified surfaces

The static contact angle was measured with a research goniometer (Ramé-Hart, Netcong, NJ). A 2µl droplet of deionized water was placed on the sample surface and the resulting angle read. All measurements were done in triplicate. Analysis of the surface chemistry was done using attenuated total reflectance (ATR) FTIR (Nicolet 6700, Thermo Electron, Madison, WI), with the sample placed on a single bounce 45° Ge crystal (Smart Performer, Thermo Electron).

### 2.4 Photografting

A “graft-from” technique was used to grow various layers on the SU-8 surface (Figure 1), starting with the formation of a surface bound initiator. The addition of a surface bound initiator molecule is done via a hydrogen abstraction technique [8]. Newly prepared SU-8 was soaked in a 5% (w/w) HCPK in ethanol solution and later place in a nitrogen filled glovebox. UV irradiation (UV LED, 27 mW/cm<sup>2</sup> at 375 nm emission, Opto Technologies, Wheeling, IL) of the SU-8 surface was performed for 30 minutes (total exposure of 48,600 mJ/cm<sup>2</sup>), resulting in the formation of surface bound photoinitiator. Once reacted, the modified samples were washed with ethanol to remove any excess HCPK, and allowed to dry. Grafted hydrogel layers were then grown on the substrate by covering the modified SU-8 samples with a mixture of monomer (HEMA, PEGMA) and/or crosslinker (TEGDMA, PEGDMA). Polymerization followed when the material and monomer mixture were exposed to UV irradiation again in a nitrogen atmosphere. These resulting hydrogel modified materials were then washed with DI water, dried, and then analyzed.

## 2.5 Micropatterning

The photoinitiator modified SU-8 materials were covered with a thin film of monomers by spin-coating. All monomer solutions used in the experiment were bubbled with nitrogen for 20 minutes to remove oxygen. A chromium-plated glass mask was then placed on the top of the sample tightly. The sample was then irradiated with UV light through a collimating lens for 30 min at an energy dose of  $9,900 \text{ mJ/cm}^2$  ( $5.5 \text{ mW/cm}^2$  at  $365 \text{ nm}$ ). Finally, the exposed sample was developed and washed by ethanol to get rid of the unreacted monomers.

The resulting patterns were examined several ways. The height and profile of the pattern was determined by a profilometer (Alpha-step 200). SEM images were taken (Hitachi S-570 SEM) to examine the pattern formation on SU-8 surface. Before imaging, a thin layer of gold and palladium was sputtered on the sample for 30 seconds to prevent electron oxidation corrosion for polymer pattern.

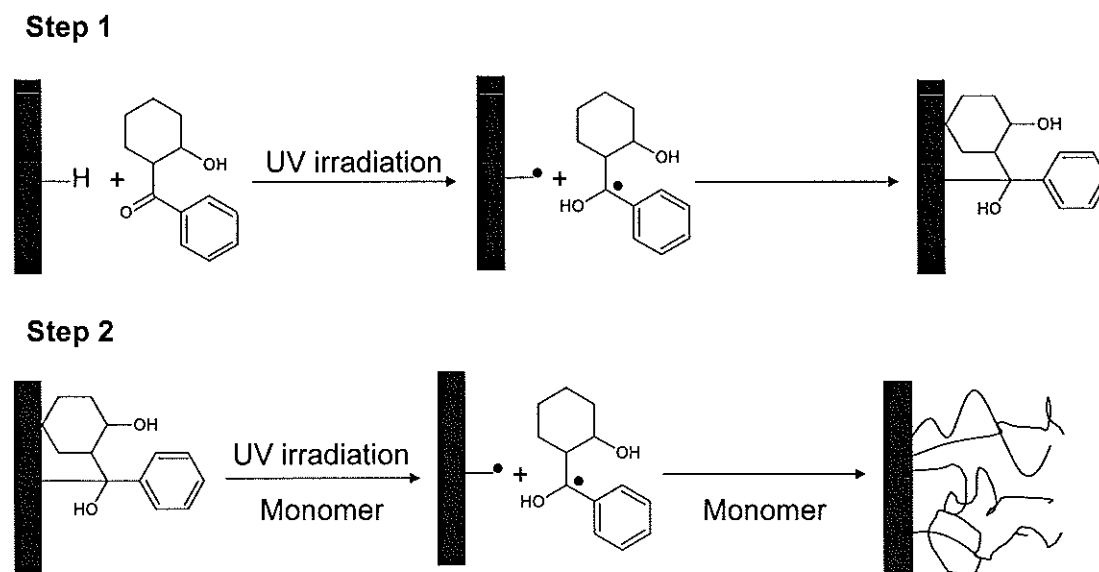


Figure 1 Schematic diagram for the photoinduced graft polymerization of monomer onto a SU-8 surface.

### 3. DISCUSSIONS

#### 3.1 Effect of hydrogel composition on wettability

Various amounts of crosslinker were studied to determine any possible effect on wettability. Hydrogel modified SU-8 samples were prepared using various ratios of HEMA: TEGDMA, ranging from 2 to 10% TEGDMA. Greater amounts of the hydrophilic HEMA monomer resulted in surfaces with enhanced wettability (Figure 2). In general, lower degrees of crosslinking allow for greater water uptake in hydrogels [10]. This result was confirmed in these experiments, as it was ultimately determined that a 98% HEMA: 2% TEGDMA (w/w) mixture provided the best wettability, as reflected by the static contact angle measurement of  $36 \pm 1^\circ$ .

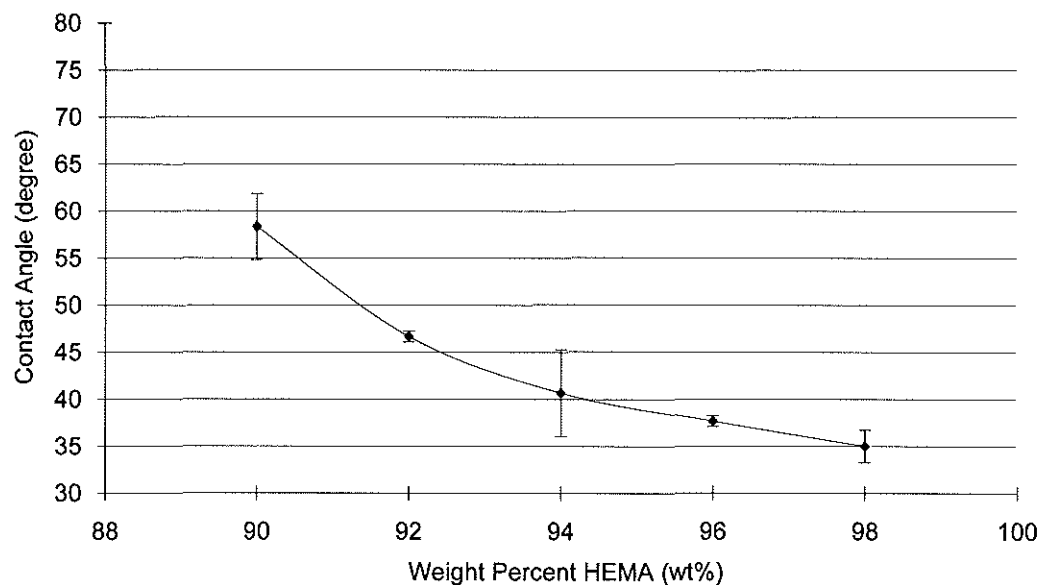


Figure 2 Static water contact angle decreases with increasing percentage of HEMA in prepolymerization mixture.

### 3.2 Effect of polymerization time

It should be noted that surface initiation techniques rely on monolayers of reactive species, which means inherently low initiator concentrations and therefore slow reaction kinetics. This disadvantage is outweighed, however, by the great deal of spatial control gained when coupling a “graft from” technique with photolithographic processing. In order to determine optimal reaction times, we studied the dynamic growth of the hydrogel layer. Before modification, the static contact angle of a freshly prepared SU-8 sample was measured as  $79 \pm 1^\circ$ . One specific hydrogel formulation (95% HEMA, 5% TEGDMA) was used to study the dynamic growth of the grafted hydrogel layer. Samples were created with varying reaction times, ranging from 10 to 50 minutes, and the resulting contact angles measured (Figure 3). The data is best described as a monotonic decrease in contact angle as a function of time. The wettability increases rapidly in the first few minutes but then slows as surface initiation sites are consumed (monomer is present in great excess and is not likely to limit the reaction).

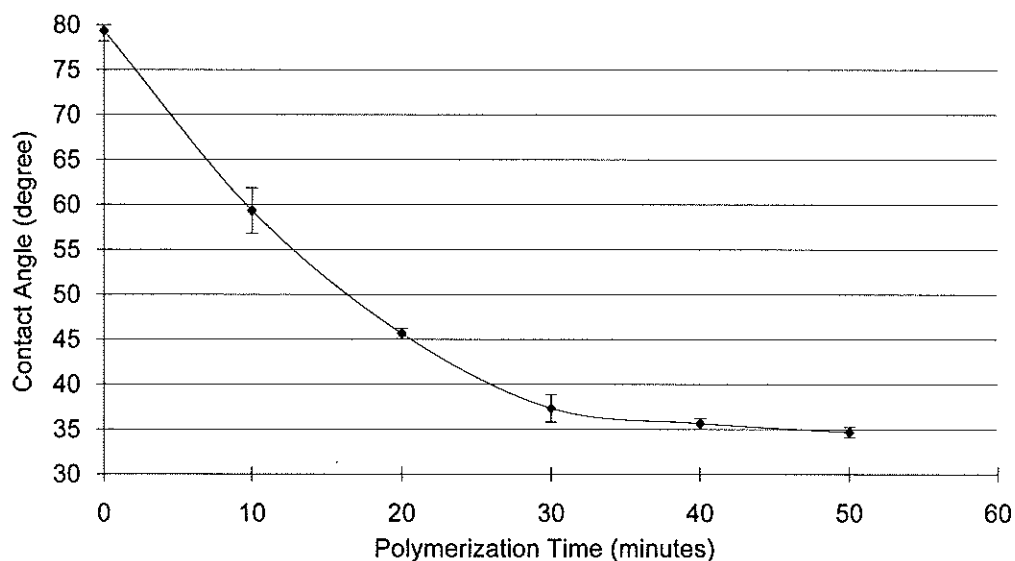


Figure 3 Influence of polymerization reaction time on surface wettability for 95% HEMA hydrogel on SU-8.

Verification of this result was accomplished through a surface chemical detection technique, ATR-FTIR (Figure 4). Shown are unmodified SU-8 substrate 4(d), surface after 10 minutes of polymerization 4(c), surface after 50 minutes of polymerization 4(b), and a reference spectrum of a bulk prepared hydrogel (also 95% HEMA: 5% TEGDMA). After 50 minutes of polymerization, the SU-8-grafted-hydrogel spectrum appears nearly identical to that of the bulk hydrogel material, indicating the presence of a distinct pHEMA layer.

### 3.3 PEG surface layer

PEG is a molecule of substantial interest and is frequently used to improve the biocompatibility of materials. Modification of the SU-8 surface with PEG macromonomers resulted in a substantial decrease in the static water contact angle. As shown in Table 1, the average static contact angle for PEGDMA modified SU-8 is  $8 \pm 1^\circ$ , which indicates high surface wettability. The PEGMA modified surface also shows a significant contact angle decrease from  $79 \pm 1^\circ$  to  $23 \pm 1^\circ$ . The significant decrease in contact angle indicates that PEG chains have been successfully attached to SU-8 surface and make it distinctly wettable. These results were later confirmed by the ATR-FTIR spectra of modified SU-8 surface (Shown in Figures 5-7).

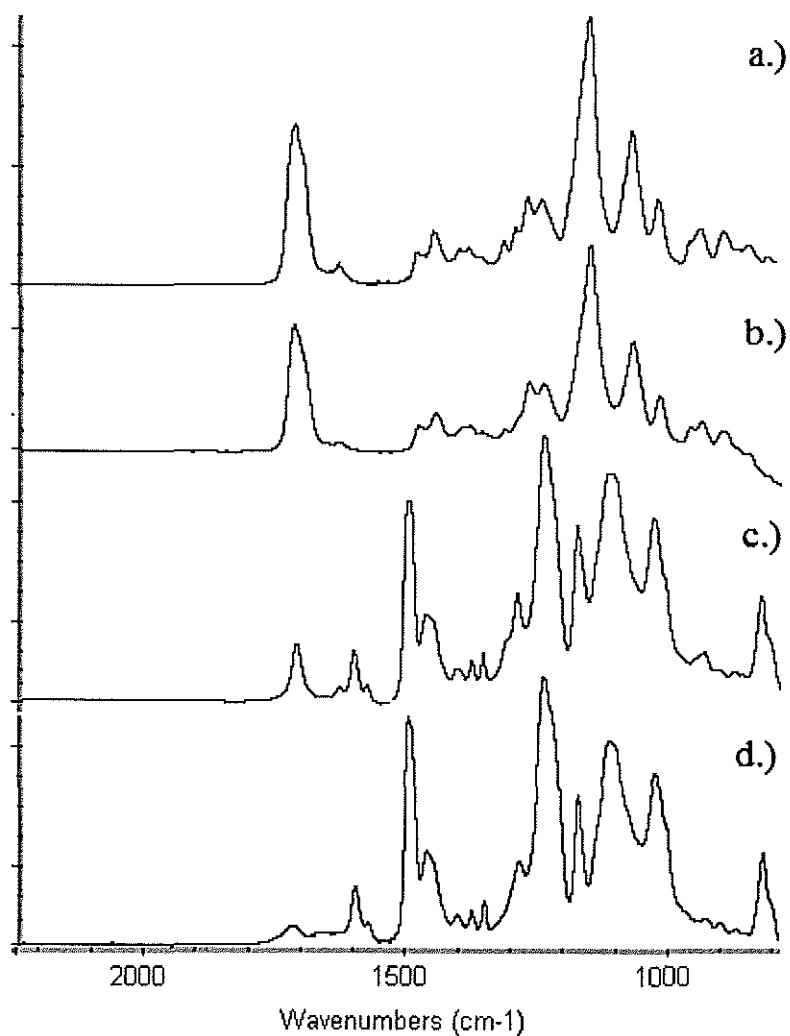


Figure 4 ATR-FTIR spectra: pHEMA photo-grafting on SU-8 surface

- a.) Reference spectrum of hydrogel (95% HEMA, 5% TEGDMA).
- b.) Surface after 50 minutes of polymerization.
- c.) Surface after 10 minutes of UV initiated polymerization.
- d.) Unmodified SU-8 surface.

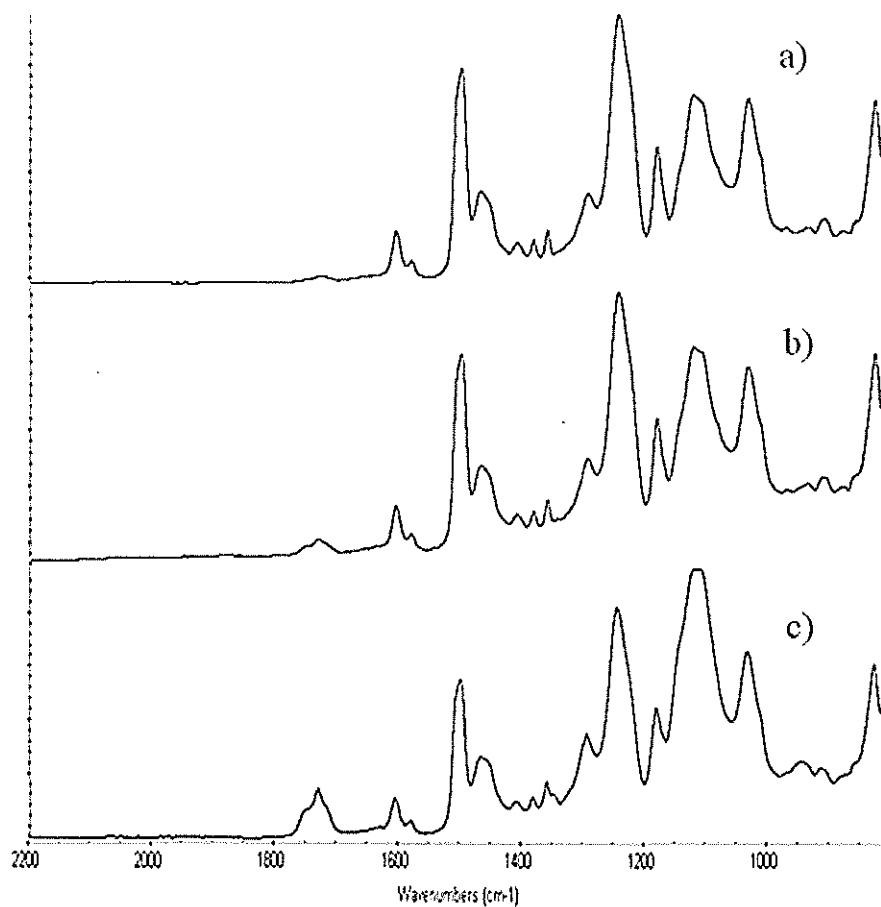


Figure 5 ATR-FTIR spectra: PEGDMA hydrogel on SU-8 surface

- a) Unmodified SU-8 surface after development and hard bake
- b) Scan of initiator HCPK bound SU-8 surface
- c) Surface after 30 minutes of polymerization of PEGDMA on SU-8 surface

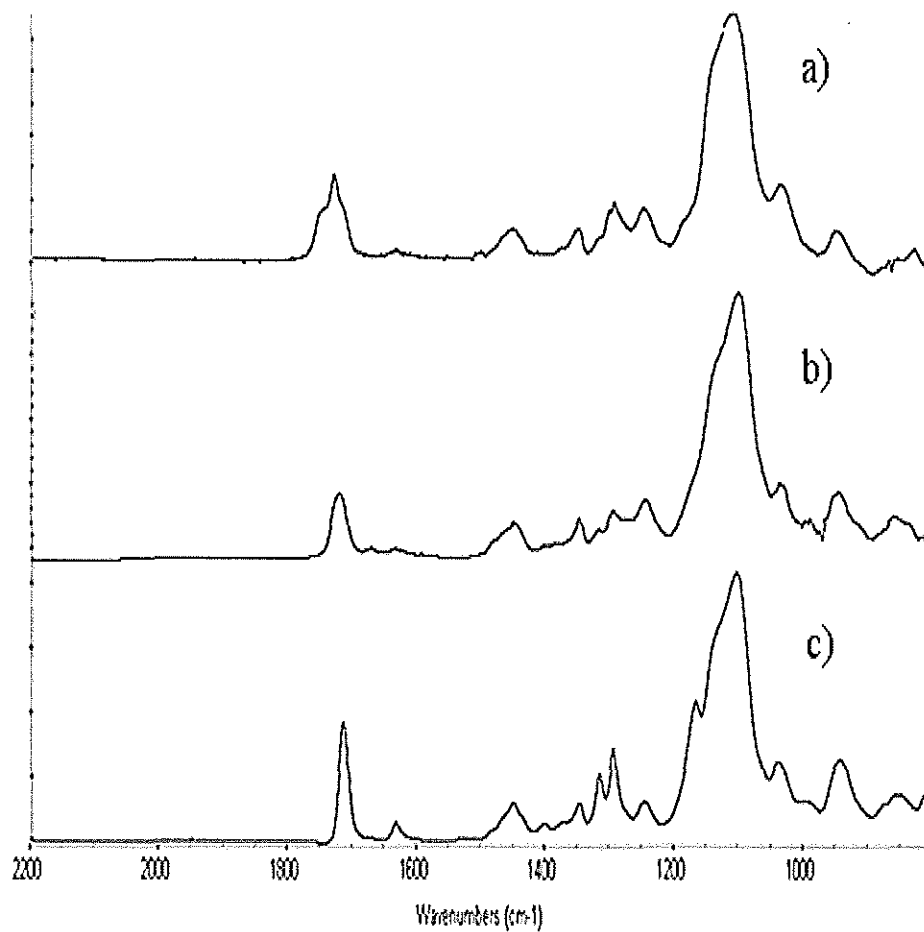


Figure 6 ATR-FTIR subtraction spectra: PEGDMA hydrogel on SU-8 surface

- a) Subtraction spectrum of PEGDMA  
(reference spectrum of initiator HCPK bound SU-8 surface).
- b) Polymerized PEGDMA hydrogel (99%PEGMA+1% HCPK)
- c) PEGDMA monomer ( $M_n=875$ )

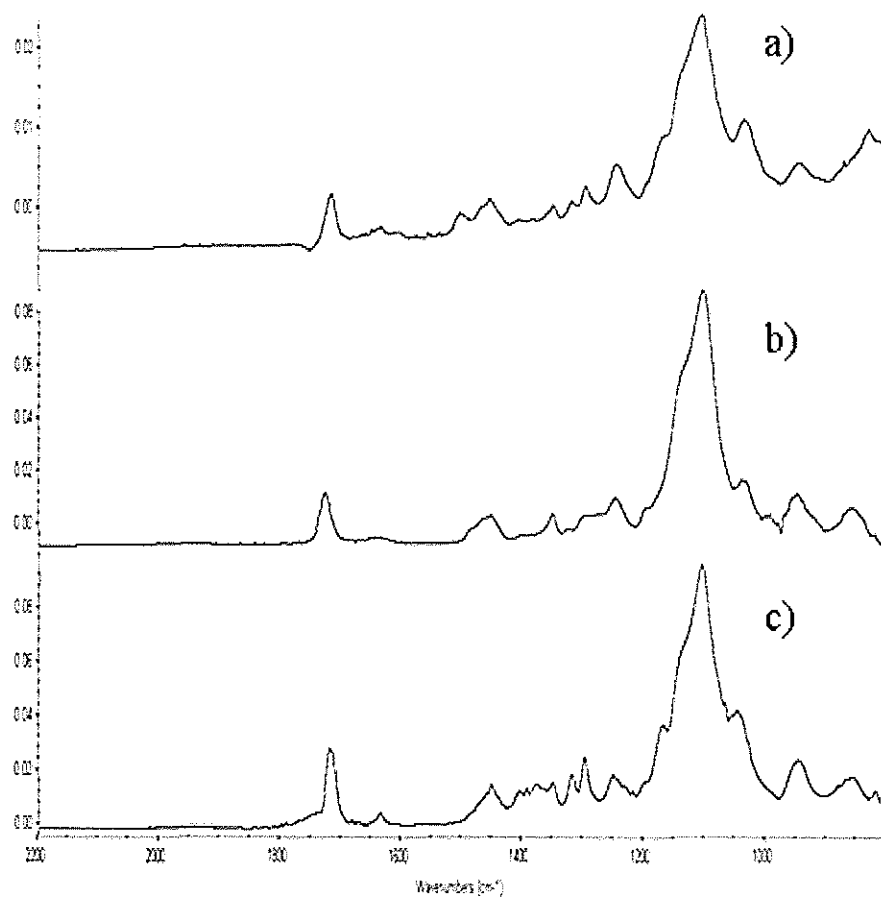


Figure 7 ATR-FTIR subtraction spectra: PEGDMA hydrogel on SU-8 surface

- a) Subtraction spectrum of PEGMA  
(Reference spectrum of initiator HCPK bound SU-8 surface).
- b) Polymerized PEGMA hydrogel (99%PEGMA+1% HCPK)
- c) PEGMA monomer (Mn=475)

Table 1 Contact angle measurement of PEG modified SU-8 surface

Materials	Measured Contact Angle
Fresh SU-8 substrate	$79 \pm 1^\circ$
PEGDMA hydrogel on SU-8	$8 \pm 1^\circ$
PEGMA hydrogel on SU-8	$23 \pm 1^\circ$
95% PEGMA+5% PEGDMA hydrogel on SU-8	$22 \pm 2^\circ$

The results were confirmed using ATR-FTIR. The ATR-FTIR spectra of fresh and PEGDMA modified SU-8 is shown in Figure 5 and 6. In Figure 5(c), the characteristic adsorption band for O-C=O stretch ( $1727 \text{ cm}^{-1}$ ), attributable to the methacrylated groups in the grafted PEGDMA polymer appear stronger than that in Figure 5(a). Another characteristic adsorption band for C-O stretch ( $1100 \text{ cm}^{-1}$ ) was also strengthened in Figure 5(c) compared with the spectra of blank SU-8. These two differences strongly indicate that PEGDMA chains have been successfully covalently bound to SU-8 surface. To further confirm this result, a subtraction spectrum between PEGDMA modified and HCPK initiated SU-8 was determined. As shown in Figure 6, the PEGDMA subtraction spectrum is nearly identical to that of the reference spectrum, indicating the formation of PEGDMA layer. The difference between the spectrum in Figure 6(a), (b) and Figure 6(c) shows that majority of PEG monomers were polymerized on the SU-8 surface. The similar conclusion can be reached by analysis of Figure 7. Shown are subtraction spectrum between PEGDMA modified and fresh SU-8 7(a), Polymerized PEGMA hydrogel (99% PEGMA+1% HCPK) 7(b), and PEGMA monomer ( $M_n=475$ ) 7(c). ATR-FTIR confirm the presence of poly(PEGMA) on the SU-8 surface.

### 3.4 Verification of proposed reaction

Table 2 Static water contact angle measurements of HEMA modified SU-8 for triple repeats in air and in oxygen free environments to verify surface initiator role

	without HCPK treatment	without UV irradiation	with HCPK treatment and UV irradiation
Air	79±1°	78±1°	75±3°
Oxygen free environment	78±3°	77±2°	35±1°

\* Contact angle of fresh SU-8: 79±1°

All samples received the same UV dosage and HEMA amount during the polymerization step. Only the addition of surface bound photoinitiator was altered:

“without HCPK treatment”: Monomer and fresh SU-8 were exposed to UV light without the initial step of adding surface bound photoinitiator

“without UV irradiation” SU-8 material was soaked in photoinitiator solution but no UV irradiation was used for activation.

“with HCPK treatment and UV irradiation”: SU-8 was modified as described previously – photoinitiator was present and activated with UV light

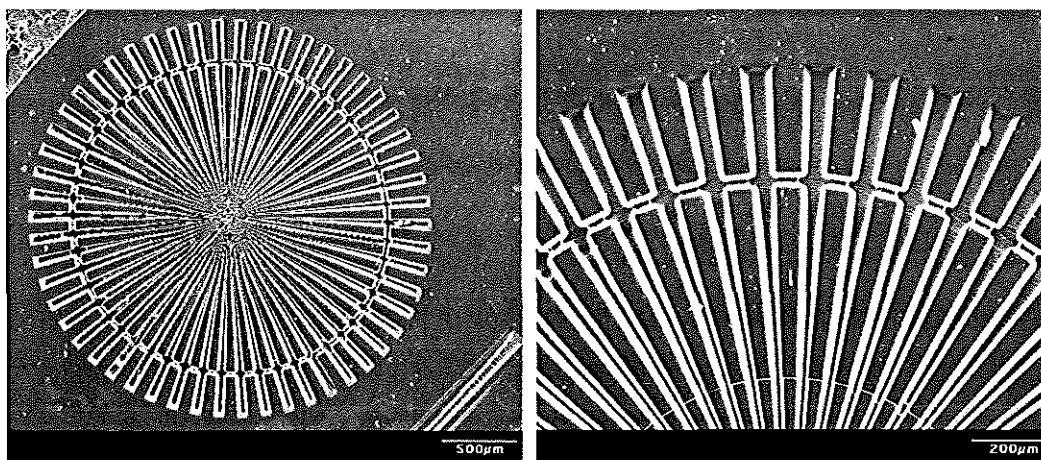
A series of comparative experiments were conducted to verify the proposed mechanism of Figure 1, and the results are shown in Table 2. Static water contact angle measurements were made on samples to illustrate the need for the various steps. In each case, polymerization was done to produce a grafted pHEMA film, with any unreacted monomer removed via washing. First, the need for an oxygen free environment is shown through loss of wettability when the steps were conducted in air. Next, the role of the surface bound initiator was established through a set of experiments. The contact angle of irradiated pHEMA on SU-8 in the absence of HCPK was not significantly different than that of freshly prepared SU-8, indicating the need for photoinitiator. Next, a set of experiments were conducted where the material was incubated in photoinitiator solution

without activation with UV irradiation. This set also produced materials with no significant wettability enhancement over the control (freshly prepared SU-8) material. These results verified that the reaction proceeded as desired and that addition of activated photoinitiator is necessary for film formation.

### **3.5 Photopatterning of PEGDMA**

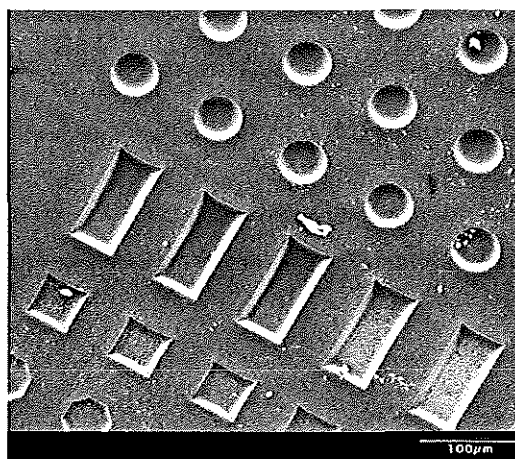
In this experiment the monomer PEGDMA was spin-coated onto an activated SU-8 surface at 600 rpm for 15 seconds. The sample was then covered with a patterning mask and exposed to UV light through a collimating lens for 30 min. The mask used here contained many various features. After exposure, PEGDMA patterns were developed with ethanol and dried to constant weight. Then samples were then stored in D. I. water for two days to observe if any delamination would occur (none seen). As these films are significantly hydrophilic and swellable, lack of delamination indicated a strong bond between the substrate and grafted film. SEM images of the PEGDMA patterns on are shown in Figures 8(a) and (b).

The same procedure was also used with a test mask containing circles with diameter of 50  $\mu\text{m}$ , rectangles (50  $\mu\text{m}$  wide and 100  $\mu\text{m}$  long), and 50  $\mu\text{m}$ ×50  $\mu\text{m}$  squares. Uniform hydrogel patterns are shown in Figure 8(c) and clearly demonstrate the precision that was attained with this technology. Profilometry results reveal that the height of patterns was approximately 7  $\mu\text{m}$ .



(a)

(b)



(c)

Figure 8 Scanning electron micrographs of PEGDMA ( $M_n=875$ ) gel microstructures on SU-8 surface.

- (a) Wheel-like PEG microstructure consists of 50  $\mu\text{m}$  wide rod (at outer side)
- (b) SEM image of wheel-like PEG microstructure (tilt angle= $60^\circ$ )
- (c) SEM image of photopatterned grafted layer on SU-8 surface (tilt angle= $30^\circ$ )

#### **4. CONCLUSIONS**

We have presented a new technique to improve the wettability of negative-tone photoresist, SU-8 used to build the microfluidic channels on silicon wafer. This technique is amenable to photolithography and therefore affords spatial control. This technique also attempts to avoid any harsh conditions (strong oxidizers, plasma, high temperatures, etc.) that are incompatible with various molecules of interest; especially proteins (enzymes, antibodies, etc.) used in manufacture of bioMEMS devices. The ability to grow covalently bound polymer layers opens a broad range of modification techniques to integrate functional components for bioanalytical device applications. These components include photografted hydrophilic polymer brushes for reduction of protein adsorption or incorporation of various biorecognition layers such as enzyme immobilized hydrogel.

#### **ACKNOWLEDGMENTS**

This work was funded by grants from the NSF (ECS0427360) and NIH (EB006611-01) as well as by the Intelligent System Center, University of Missouri-Rolla.

## REFERENCES

- [1] Madou M 1997 *Fundamentals of Microfabrication* (Boca Raton, FL: CRC Press)
- [2] Lorenz H, Despont M, Fahrni N, Brugger J, Vettiger P, Renaud P 1998 High-aspect-ratio, ultrathick, negative-tone near-UV photoresist and its applications for MEMS *Sensors and Actuators A* **63** 33-9
- [3] Bilenberg B, Hielson T, Clausen B, Kristensen A, 2004 PMMA to SU-8 bonding for polymer based lab-on-a-chip systems with integrated optics *J. Micromech. Microeng.* **14** 814-818
- [4] Wu C L, Chen M H, and Tseng F G, Oct. 2003 SU-8 hydrophilic modification by forming copolymer with hydrophilic epoxy molecule *7th International Conference on Miniaturized Chemical and Biochemical Analysis Systems*, Squaw Valley, CA, USA, 1117-20
- [5] Nordstrom M, Marie R, Calleja M, and Boisen A 2004 Rendering SU-8 hydrophilic to facilitate use in micro channel fabrication *J. Micromech. Microeng.* **14** 1614-7
- [6] Yuli Wang, Jeng-Hao Pai, Hsuan-Hong Lai, Christopher E Sims, Mark Bachman, G P Li, and Nancy L Allbritton 2007 Surface graft polymerization of SU-8 for bio-MEMS applications *J. Micromech. Microeng.* **17** 1371-80
- [7] Tseng F-G, Lin K-H, Hsu H-T, and Chieng C-C 2004 A surface-tension driven fluidic network for precise enzyme batch-dispensing and glucose detection *Sensors and Actuators A* **111** 107-117
- [8] Walther F, Davydovskaya P, Zurcher S, Kaiser M, Herberg H, Gigler A M and Stark R W 2007 Stability of the hydrophilic behavior of oxygen plasma activated SU-8 *J. Micromech. Microeng.* **17** 524-31
- [9] Sung C, Sobarzo M R and Merrill E W 1990 Synthesis and characterization of polymer networks made from poly(ethylene oxide) and polysiloxane *Polymer* **31** 556-63
- [10] Kim P, Jeong H E, and Suh K Y *Fabrication of non-biofouling polyethylene glycol micro- and nanochannels* 3<sup>rd</sup> Korea-US NanoForum, Seoul, Korea, April 3-4, 2006
- [11] Lan S, Mandana V and Zhang M 2005 Surface modification of silicon and gold-patterned silicon surfaces for improved biocompatibility and cell patterning selectivity *Biosensors and Bioelectronics* **20** 1697-708
- [12] Voskerician G, Shive M S, Shawgo R S, Recum H V, Anderson J M, Cima M J and Langer R 2003 Biocompatibility and biofouling of MEMS drug delivery devices *Biomaterials* **24** 1959-67

- [13] Ma H, Davis and R H, Bowman C N 2000 A novel sequential photoinduced living graft polymerization *Macromolecules* **33** 331-5
- [14] Peppas N A, Huang Y, Torres-Lugo M, Ward J H, and Zhang J 2000 Physicochemical foundations and structural design of hydrogels in medicine and biology *Annu. Rev. Biomed. Eng.* **2** 9-29
- [15] Fornasiero F, Krull F, Prausnitz J M and Radke C J 2005 Steady-state diffusion of water through soft-contact-lens materials *Biomaterials* **26** 5704-16
- [16] Arica M Y and Hasirci V N 1987 Immobilization of glucose oxidase in poly(2-hydroxyethyl methacrylate) membranes *Biomaterials* **8** 489-95
- [17] Arica M Y and Hasirci V 1993 Immobilization of glucose oxidase: a comparison of entrapment and covalent bonding *J Chem. Technol. Biotechnol.* **58** 287-92
- [18] Harris J M and Zalipsky S 1997 *Poly(ethylene glycol) chemistry and biological application* (Washington DC: American Chemical Society)

## II. Sensor application of poly (ethylene glycol) diacrylate hydrogel chemically anchored on polymer surface

### ABSTRACT

A poly (ethylene glycol) (PEG)-rich hydrogel was used as a photopatternable matrix material for the immobilization of fluorophore for optical oxygen sensor application. This hydrogel was chemically anchored on negative-tone photoresist SU-8 surface through a free radical reaction in which 1-hydroxycyclohexyl phenyl ketone (HCPK) served as the surface bound photoinitiator. The optical oxygen detection scheme was based on the quenching behavior of a fluorophore, dichlorotris (1, 10-phenanthroline) ruthenium (II) hydrate, toward dissolved oxygen molecules. The simplified optical oxygen sensor using SU-8 photoresist as platform exhibited a reversible Stern-Volmer response to oxygen at the optimal concentration of 2.81mM ruthenium complex entrapped in poly (ethylene glycol) diacrylate-based-hydrogel. It also showed excellent storage stability and maintained 95% of its initial relative sensitivity even after two months storage in D.I. water. Furthermore, cylindrical PEG-rich hydrogel membrane with ruthenium complex entrapped was successfully anchoring inside the channel after bonding process of SU-8 channel with our novel chemical anchoring technique. All of these indicate that the chemical anchoring technology of biocompatible, patternable polymerized PEG rich membranes for SU-8 surface is a useful method for implementing microfluidic sensing membrane within polymeric channel structures.

### 1. INTRODUCTION

In the last decade there has been a growing interest in the development of microfluidic channels devices with dimension of tens to hundreds of micrometers for lab-on-a-chip technology [1]. In order to cut the cost and shorten the analysis time, optical sensors constructed based on microfluidic channels with sensing elements built within them attract more and more attention. One important application of optical microfluidic sensors is in the monitoring of dissolved oxygen concentration, with important uses in chemical, biological and environmental settings. Such kind of sensor has many needed

advantages, like no consumption of the oxygen molecules, no need for reference electrodes, and no electrical interference compared with electrochemical oxygen sensors [2]. Most of them are designed based on a common detection mechanism, which is to employ the fluorescent quenching behavior of an analyte responsive fluorophore immobilized in a matrix placed in the microfluidic channels [3]. Therefore, choosing the suitable material for microfluidic channels and matrix as well as immobilization of the optically transparent structure matrix within the channels become three main concerns for sensor fabrication in this work.

Traditionally, many microfluidic devices are fabricated with silicon, if transparent setups are necessary, with glass, which require complex, time-consuming and expensive process. In recent years, negative-tone photoresists have become popular materials in the fabrication of microdevices as a replacement for glass or silicon substrates due to less cost of manufacture. The epoxy-based, photopolymer known as SU-8 has found increasing use as a structural material in microfluidic devices [4]. Besides its special characteristics like ability to produce high aspect ratio microstructures and compatibility with conventional microfabrication techniques [5], it also has many properties that make it attractive as structure materials for optical sensors. The properties include nontoxicity, excellent optical transparency, good mechanical strength [6, 7] and low temperature require for adhesive bonding process for SU-8 channel fabrication [8, 9]. Thirdly, unlike the widely used microfluidic channel material, PDMS, SU-8 is less oxygen permeable, which is an important characteristic for oxygen measurement. The attractiveness of SU-8 photoresist as a structure material for the fabrication of fluidic optical oxygen sensor can be further enhanced if we can chemically anchor sensing elements in specific regions by simply modifying the SU-8 surface within fluidic channel after bonding process.

Sensing elements for this sensing system have two important parts: one is fluorophore which is optical sensitive to the specific analyte; while the other is the matrix which can entrap the fluorophore and allows for unhindered diffusion of the analyte. A lot of efforts have been put on developing new matrix materials and investigating their performances. Issues regarding oxygen permeability, fluorophore solubility within the matrix, leaching of the fluorophore must be carefully considered before optical oxygen sensor matrix design since quality of sensing elements is closely related to the later

oxygen measurement. Previous optical oxygen sensor studies have utilized various materials as matrix to immobilize the fluorophore and two of most widely used materials are sol-gel and silicone rubber [10]. Considering optimum biocompatibility, and better solubility and entrapment of the commonly used fluorophore, ruthenium complex in matrix, PEG-DA was employed here as matrix material [4, 11-14].

Although surface modification techniques of SU-8 by using PEG polymer have been extensively reported, most of them are restricted to surface properties changing of SU-8. Wang et al. [15, 16] reported two methods for the photografting of poly (ethylene glycol) (PEG) from the surface of SU-8 photoresist. In the first method, PEG chains were grafted from the SU-8 surface through a free radical reaction using the photoacid generator triarylsulfonium hexafluoroantimonate as a photoinitiator [15]. Alternatively, surface exposed epoxy groups of SU-8 photoresist were chemically converted into hydroxyl groups, which then served as initiation sites for the graft polymerization of PEG on SU-8. Both of the steps are catalyzed by cerium (IV) ammonium nitrate in the acid environment [16]. Desai et al [17] used aminopropyltriethoxysilane as a bridge to couple the PEG monomers to SU-8 surface, whose epoxy groups was opened by using concentrated sulfuric acid. The primary focus of these works was to enhance the biofunctionality and wettability properties of SU-8 rather than anchor relative thick patternable hydrogel structures, which is necessary for either electrochemical or optical sensing application. The photoinitiator HCPK was covalently bonded on the specific areas of SU-8 surface through a hydrogen abstraction reaction, and these molecules later served as chemical anchoring sites for the patterned bulk PEG membrane [18].

In this study, an optical oxygen fluidic sensor was constructed by chemically anchoring PEG-rich hydrogel matrixes within the SU-8 channel after bonding process through the photo initiation procedure developed previously [18]. A ruthenium complex, dichlorotris (1, 10-phenanthroline) ruthenium (II) hydrated was chosen as the fluorophore for oxygen detection due to its efficient luminescence, relatively long excited-state lifetime, and significant quenching behavior in the presence of oxygen molecules [3]. Detection characteristics including relative sensitivity, reversibility and long-term stability were investigated and dissolved oxygen content measurement was tested by using a truly integrated optical oxygen SU-8 fluidic sensor.

## 2. EXPERIMENTAL

### 2.1 Materials

Poly (ethylene glycol) diacrylate (PEG-DA) with an average molecular weight of 575, HCPK photoinitiator, the oxygen sensitive fluorescent compound ruthenium complex, dichlorotris (1, 10-phenanthroline) ruthenium (II) hydrated 98% and toluene were purchased from Sigma-Aldrich (St. Louis, MO). Acetone, methanol and isopropanol were obtained from Fisher Scientific (Fair lawn, NJ). The negative tone photoresist SU-8 (formulation 2050) and SU-8 developer were purchased from MicroChem (Newton, MA). 700  $\mu\text{m}$  thick 4 inch borofloat glass wafers were obtained from University Wafer (South Boston, MA).

### 2.2 Surface immobilized oxygen-sensitive hydrogel membrane formation

*2.2.1 Preparation of SU-8 films.* Negative photomasks for 1 cm $\times$ 1 cm square SU-8 patterns were designed using the Microsoft Visio software and printed on Mylar sheets. These sheets were attached to transparent square glass plates to form photomasks for the subsequent photolithography step.

A 4 inch glass wafer was cleaned using acetone, methanol, and then D.I. water for 3 minutes, followed by drying with air for 30 seconds. Next, the glass wafer was dehydrated on a hotplate at 150  $^{\circ}\text{C}$  for 10 minutes. A 75  $\mu\text{m}$  thick SU-8 film was formed on the glass wafer by spin-coating at 500 rpm for 10 seconds, followed by 2000 rpm for 30 seconds using a single wafer spin processor (WS-400E-6NPP/LITE, Laell Technologies Corporation). Directly after the spin-coating procedure, the samples were put onto the hotplate at 65  $^{\circ}\text{C}$  for 3 minutes and then at 95  $^{\circ}\text{C}$  for 9 min in the softbake step. The SU-8 patterned films were prepared through exposure to a collimated UV light source ( $\sim 5.5 \text{ mW/cm}^2$  at 365 nm) for 60 seconds. The total exposure energy dose was 330  $\text{mJ/cm}^2$ . After irradiation, the postbake step was carried out on a hotplate at 65  $^{\circ}\text{C}$  for 1 hour. After slowly cooling down to the room temperature, the patterned SU-8 sample was soaked in SU-8 developer for 7 minutes and then rinsed with isopropanol to remove any unreacted SU-8 residue. Finally, the sample was dried under vacuum for 12 hours.

*2.2.2. Chemical anchoring procedure.* The glass wafers with SU-8 coatings were immersed in a 5 % (w/w) HCPK in ethanol solution for 10 minutes and later placed in nitrogen atmosphere to prevent any oxygen quenching effects. The photoinitiator was covalently bound to the SU-8 surface through 30 minutes irradiation by uncollimated UV light ( $\sim 26.5$  mW/cm<sup>2</sup> at 365 nm) via a hydrogen abstraction technique, as detailed previously [18]. Once irradiated, the photoinitiated SU-8 film coated glass wafers were immersed in ethanol overnight to remove any unbound photoinitiators and dried in a vacuum oven for 12 hours. The glass wafer was later cut into 1.5 cm $\times$ 1.5 cm small pieces, each of them with one intact initiated SU-8 pattern on the top surface.

The ruthenium complex solution was made in a 4:1 (v: v) mixture of methanol and toluene. PEG-DA was dissolved in deionized water at a 60% (w/w) prior to polymerization, with the large water content being used to produce gels with an open structure to facilitate analyte diffusion. Previously published work showed that 40% water content is optimal for the diffusion of small molecules through the PEG-DA matrix [14]. Finally, the ruthenium complex solution was added to the diluted PEG-DA solution to make a 1:10 (v:v) mixture. This mixture was bubbled with nitrogen gas for 30 minutes before polymerization to remove oxygen molecules.

As shown in Fig. 1 (a), voidspace was created by using 175  $\mu$ m thick black insulation tape as a spacer layer leaving an SU-8 area of 0.5 cm  $\times$  0.5 cm. Immediately after the ruthenium mixture was saturated with nitrogen, 0.01 ml of PEG-DA / ruthenium mixture was allowed to fill the space between the glass cover and the photoinitiated SU-8 film. A glass cover was secured tightly on the top of the sample to avoid any oxygen quenching effect on polymerization. The excess liquid around the edge of the tape was cleaned with Kimwipes.

This glass cover/PEG-DA/SU-8 assembly was placed on the sample stage of a mask aligner (CA-800, Cobilt, Computervision) and exposed to UV light ( $\sim 5.5$  mW/cm<sup>2</sup> at 365 nm) for 30 minutes. After the irradiation, the assembly was pulled apart, leaving the ruthenium loaded PEG-DA covalently bound to the SU-8 film (shown in Fig. 1 (b)). The sensor was placed in water for 12 hours before the fluorescence intensity measurement to allow for the removal of any untrapped ruthenium complex or unreacted monomers.

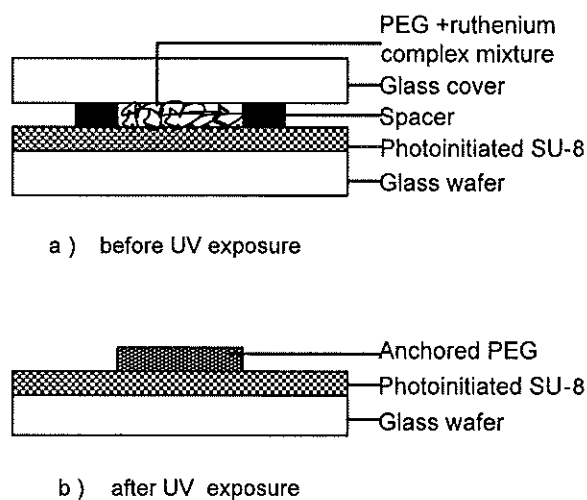


Fig.1. Preparation of oxygen-sensitive hydrogel anchored on SU-8 surface. a) Ruthenium complex and PEG-DA monomers mixture filled out the space of glass cover/spacer/SU-8 assembly; b) PEG-DA membrane was chemically anchoring on the photoinitiated SU-8 surface after UV exposure.

*2.2.3. SU-8 channel fabrication.* A transparent glass microscope slide used as glass substrate was cleaned in Acetone, Methanol and D.I. water for 3 minutes respectively and dried in air for 30 seconds after each step. It was then dehydrated on a hotplate at 200 °C for at least 15 minutes immediately prior to use. 4 ml SU-8 2050 was spin-coated on the dehydrated glass slide at 500 rpm for 10 seconds, followed by 2000 rpm for 30 seconds to produce a 75  $\mu\text{m}$  thick SU-8 layer. This SU-8 layer was soft-baked on a hotplate at 65 °C for 3 minutes followed by holding at 95 °C for 9 min and then put on the Mask Aligner (Karl Suss MA6, Suss MicroTech) stage to cool down to room temperature. This SU-8 layer was then exposed to UV light (5.7 mW/cm<sup>2</sup>, 365nm) for 56 seconds and hard-baked on a hotplate at 95 °C for 9 min. The second SU-8 layer was spin-coated on the first one at 500 rpm for 10 seconds, followed by 1000 rpm for 30 second to produce a 125  $\mu\text{m}$  thick film. The second SU-8 layer was soft-baked on a hot plate at 95 °C for 10 min and then exposed to UV light with an appropriate mask for 88 seconds. After UV flood exposure step, this sample was post-baked using the same

receipt as for the soft-bake step. The channel structure was developed in propylene glycol methyl ether acetate (PGMEA) for 9 minutes and then rinsed with isopropanol to remove any unreacted SU-8 residue.

Another glass microscope slide at the same size used as a cover was cleaned in the same procedure as for the substrate. It was dehydrated on a hotplate at 200 °C for at least 15 minutes before the spin-coating step. 4 ml SU-8 2007, which is diluted from SU-8 2050 with SU-8 thinner, was casted on the dehydrated glass slide and spin-coated at 500 rpm for 10 seconds, followed by 2000 rpm for 30 seconds. 20 µm thick uncrosslinked SU-8 layer was formed on the glass slide after 4 min soft-baking step at 95 °C on a hotplate. After the sample cooled down to room temperature, we used Drill (Model 750, Dremel) to drill two holes used for fluidic inlet and outlet ports (As shown in Fig. 2).

The glass substrate bearing the SU-8 channel structure and the glass cover with uncrosslinked SU-8 layer were placed on a hotplate at 65 °C for 5 minutes. The glass transition temperature ( $T_g$ ) of uncrosslinked SU-8 is  $\sim 55^\circ\text{C}$  [8]. If the bonding temperature is too low (i.e. room temperature), it is hard for SU-8 layer to contract with each other since the uncrosslinked SU-8 layer is not soft enough. On the other hand, if the bonding temperature is much higher than the glass transition temperature (i.e.  $>75^\circ\text{C}$ ), the bonded SU-8 channel will be blocked since the SU-8 is so soft that it will flow into channel. In our work, the optimum bonding temperature is found to be 65 °C slightly higher than glass transition temperature of SU-8. It is considered that at that temperature, the SU-8 layer is pliable to contact with each other and therefore, most areas of the channel structure are bonded. As the glass slides were contacted, external pressure was applied to help to achieve better contact and to eliminate air bubbles since the bonding process was not carried out in vacuum environment. After the sample had cooled to room temperature, 52 seconds flood exposure through the transparent glass slide and 4 minutes post-baking step at 95 °C on a hotplate were conducted to solidify the uncrosslinked SU-8 layer, which led to a transparent sealed SU-8 channel structure.

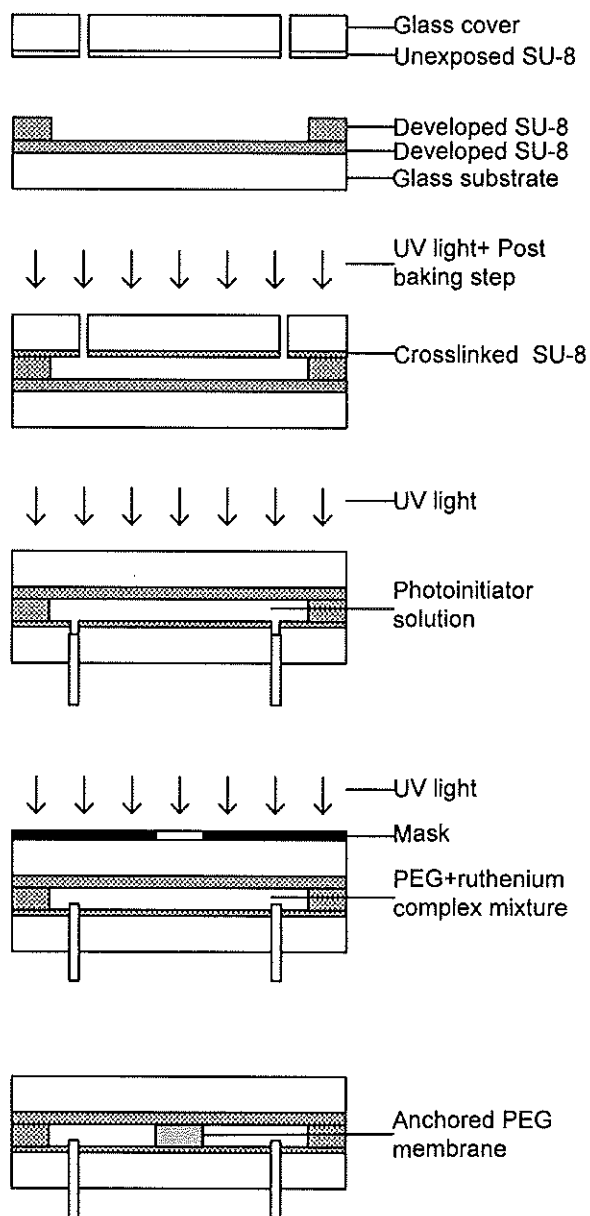


Fig 2. Fabrication process scheme of optical fluidic dissolved oxygen sensor

5 % (w/w) HCPK in ethanol solution bubbled with  $N_2$  gas for 30 minutes was injected into the channel after bonding process and exposed to UV light ( $5.7 \text{ mW/cm}^2$ , 365nm) for 30 minutes (as shown in Fig. 2). The initiator, HCPK was grafted on the channel wall surface and severed as the active site for anchoring polyethylene glycol membrane. The details about the underlying chemical reaction principle were reported in

previous publication [18]. The initiated SU-8 channel was washed thoroughly by copious ethanol in case that there is some free initiators left in channel. To achieve the chemically anchored 1 mm diameter PEG-based optical oxygen sensitive hydrogel cylindrical structure within the SU-8 channel, it was filled with N<sub>2</sub> saturated ruthenium complex-PEG mixture solution of optimum ruthenium complex concentration found through the previous experiment and then exposed to UV light (365 nm, 5.7 mW/cm<sup>2</sup>) for 30 minutes with designed mask. The precursor solution exposed to UV light formed densely crosslinked network, which entrapped the ruthenium complex, and became insoluble in D.I. water. Any polymerized PEG monomer and untrapped ruthenium complex inside the channel were later washed out by injecting copious D.I. water. In order to obtain the initial stability before the oxygen concentration measurements, the channel was flooded with D.I. water and exposed to LED light source for 12 hours before oxygen measurements.

### 2.3 Instrumentation

All luminescence intensity measurements were done with a spectrofluorometer (USB2000-FLG, Ocean Optics) and SpectraSuite software, as in an experiment setup shown in Fig. 3. The excitation and emission wavelengths of ruthenium complex, dichlorotris (1, 10 – phenanthroline) ruthenium (II) hydrate were 470 nm and 608 nm respectively. A blue LED (LS450, Ocean Optics) was used as the excitation light source. It was connected to the spectrometer by using a reflection probe (R400-7-UV-VIS, Ocean Optics) with three ends. This probe consisted of six 400 μm illumination fibers for excitation and one 400 μm read fiber to illuminate the PEG-DA matrix and to transmit emitted light to the spectrometer, respectively. The signals captured by the read fiber were high-pass filtered (>540 nm) before being read by the spectrometer.

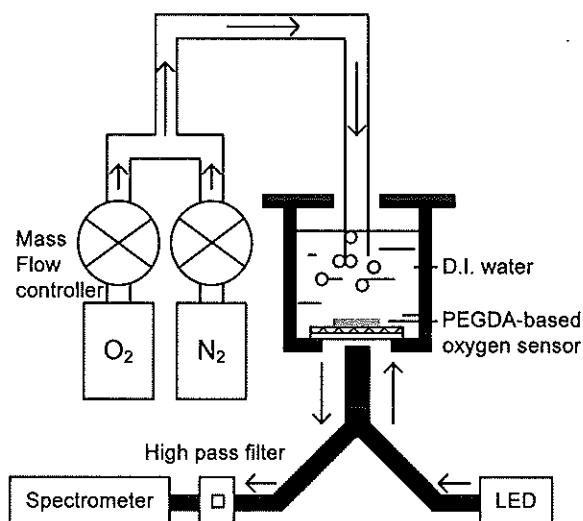


Fig. 3. Experimental setup with spectroscopic equipment and controlled gas composition for fluorescent oxygen detection.

The PEG-DA matrix with incorporated ruthenium complex was placed in a container filled with 20 ml D.I. water. A gas flow system was used to introduce oxygen and nitrogen gases into the container through the gas mass-flow controllers. Various oxygen saturation percentages were obtained by adjusting the ratio of oxygen to nitrogen gas. Fluorescence signal with respect to different oxygen concentration were captured and spectrum was displayed on the computer. The total gas flow rate was kept at 1000 sccm.

### 3. RESULTS AND DISCUSSIONS

#### 3.1 Verification of chemical anchoring scheme

To determine whether the photoinitiator HCPK played a role in initiating the polymerization reaction, a set of experiments comparing two groups of three SU-8 samples were carried out. One group of photoinitiator modified SU-8 samples and the other group of bare SU-8 samples were all subjected to the procedure of Fig. 1. To exclude the possibility that the residual photoacid generator materials remaining on the SU-8 surface was responsible for triggering the reaction, cured SU-8 films were washed

and immersed in ethanol for 12 hours before the HCPK photoinitiation procedure. Reaction with surfaces that were pro-reacted with HCPK resulted in bound PEG-DA membranes which remained attached to SU-8 despite swelling in water, while reaction with untreated surfaces led to films which were easily washed off from the surface. All samples were soaked for one day in D.I. water after polymerization. This implies that the membranes were chemically anchored on the SU-8 surface after the HCPK procedure. The thickness of poly (ethylene glycol) diacrylated-based hydrogel measured with a stylus profilometer (Alpha-step 200, Tencor Instrument) was approximately 175  $\mu\text{m}$  in hydrated state, which is the same thickness with the spacer layer.

### **3.2 Effect of photoinitiation process and initial photostability**

Highly reactive radicals are generated during the aforementioned polymerization process and it is therefore feasible that degradation of the ruthenium complex may occur. Damage to the complex would result in alteration of the fluorophore chemical structure and subsequent optical properties. To examine the photostability of the ruthenium complex during the polymerization step, a series of comparison experiments was conducted (Results listed in Table 1). Ruthenium mixture was prepared by adding 20 mg ruthenium complex, 1.0 ml PEG-DA macromonomers, 0.67 ml D.I. water, 0.03 ml toluene, and 0.13 ml methanol.

A trace of initiator HCPK was added into this mixture to trigger the polymerization reaction. This ruthenium mixture was pipetted into 6 wells on the 96 well microplates. Fluorescent intensity was measured before and after polymerization and the average values of fluorescent intensities are shown in Table 1. This comparison experiment was repeated three times. Results from Table 1 show fluorescent intensity retention of 98% (with minimal 96% and maximum 99%) after polymerization, implying that the photostability of the sensing dye was minimally affected by the free radical reaction.

Table 1. Fluorescence intensity before and after UV polymerization.

		Before (RFU*)	After (RFU*)	Percentage of fluorescence intensity retention
1st batch (n=6)	Average	1.60E+08	1.59E+08	99%
	Standard Deviation	7.00E+06	1.00E+06	
2nd batch (n=6)	Average	1.59E+08	1.53E+08	96%
	Standard Deviation	6.00E+06	1.00E+06	
3rd batch (n=6)	Average	1.60E+08	1.58E+08	98%
	Standard Deviation	8.00E+06	1.00E+06	

\* Relative Fluorescence Units: photodetector signal of spectrometer (Beckman Coulter, DTX 880) responding to fluorescence at 625 nm.

### 3.3 Spectral response and initial stability

The excitation and emission spectra of dichlorotris (1, 10 – phenanthroline) ruthenium (II) in chemically anchored PEG-DA-based membrane is shown in Fig. 4.

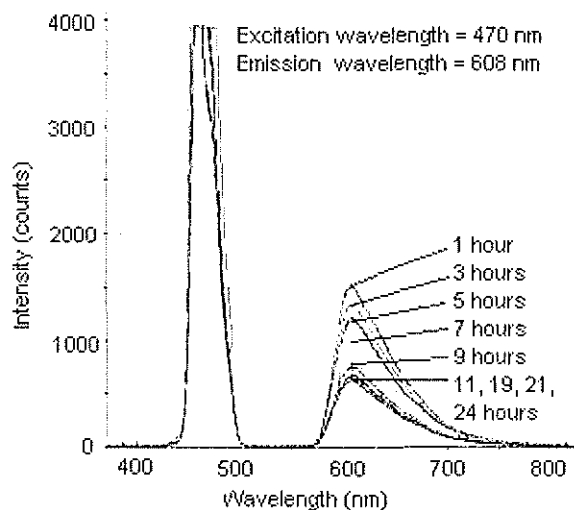


Fig. 4. Initial stability of the fluorescent emission from ruthenium complex during 12 hours after incorporation in chemically anchored PEG-DA membranes on SU-8 surface.

The excitation wavelength is 470 nm while the emission wavelength is at 608 nm respectively. An initial decrease in fluorescent emission intensity occurred when a freshly prepared sensing membrane was exposed to LED excitation source. It is considered that the reduction in emission intensity was caused mainly by the ruthenium complex leaching out of the PEG-based membrane since the natural lifetime of the fluorophore remains largely retained when they are physically immobilized in the solid matrix [3]. As shown in Fig. 4, the fluorescent intensity appeared to stabilize after 12 hours exposure to LED light source. For this reason, every hydrogel membrane was soaked in D.I. water and exposed to continuous LED light illumination for 12 hours before the first fluorescent intensity measurements.

### 3.4 Effect of ruthenium concentration on relative sensitivity

The oxygen detection by luminescence quenching can be described by the Stern-Volmer equation [3]:

$$\frac{I_0}{I} = \frac{\tau_0}{\tau} = \frac{\Phi_0}{\Phi} = 1 + K_{SV}[O_2] \quad (1)$$

$$K_{SV} = k\tau_0 \quad (2)$$

where  $I_0$  ( $\tau_0$ ,  $\Phi_0$ ), and  $I$  ( $\tau$ ,  $\Phi$ ) are the fluorescent intensities (the fluorescent lifetime, the phase shift of the fluorophores in the absence and the presence of the dissolved oxygen molecules;  $[O_2]$  is defined as percent oxygen saturation (i.e. a sample of 50% percent oxygen saturation refers to D.I. water that has been saturated with a gas comprised of 50% oxygen and 50% nitrogen by mole at atmosphere pressure) in this work.  $K_{SV}$  is the Stern-Volmer quenching constant, while  $k$  is the quencher rate coefficient.

Under isothermal and isobaric conditions,  $K_{SV}$  should remains constant, and the relationship between relative sensitivity  $I_0/I$  and  $[O_2]$  is linear. However, as shown in Fig. 5(a), the Stern-Volmer plot shows deviation from the linear relation over the full range from 0% to 100% saturation. This is a common feature of ruthenium complex physically

immobilized in matrix, serving as the sensing elements for dissolved optical oxygen sensor. Normally, the intensity decrease over continuous use is caused by photobleaching of ruthenium complex. But in our work, this phenomenon is considered not mainly caused by the degradation of the fluorophore, since no significant intensity decrease was found after initial stability process or during the 80 minutes measurements here.

The reasons for the deviation of the Stern-volmer plots are complicated. Many models were established to demonstrate the downward curvature at the range of higher dissolved oxygen. The multisite model and the non-linear solubility model are commonly used to account for this phenomenon [3]. In most cases, these two models were introduced to fit the analysis of luminescence quenching-based sensors in gas phase. Since percentage oxygen saturation in the aqueous environment is proportional to the oxygen gas portion in mixed gas phase above the D.I. water, it is considered that these two models can be used to explain non-linear Stern-volmer relationship here. According to the multisites model, the fluorophore dye has two or more quenchable sites, each with its own characteristic quenching constant. The model equation developed based two or more quenching constants is different from the Stern-volmer equation with only one quenching constant, leading to the downward curve in the plots. In the non-linear solubility model, it is assumed that fluorophore dye only has a single quenchable site, which detects the average dissolved oxygen concentration. The downward curvature is attributed to the heterogeneity of solid matrix, which will set some obstacles at the quenching binding sites, followed by the lower local O<sub>2</sub> quenching constant in the high oxygen level. In our work, both of them are considered as reasons for the deviation from the linear Stern-Volmer plots due to the multisites of ruthenium complex and heterogeneity of crosslinked network structure of PEG hydrogel.

As shown in Fig. 5(a), the deviation is more significant for the plot at the ruthenium concentration of 3.51 mM than at lower oxygen concentrations. The cluster of ruthenium complex may be the reason for this. The common chloride and perchlorate salts of the ruthenium complex are hydrophilic and thus can not disperse very well in the hydrophobic polymer matrix, like sol-gel or silicone rubber. Ruthenium complex will aggregate together in the matrix block the way of oxygen molecules towards the reactive sites of fluorophores. Therefore, less fluorescent intensity can be detected and recorded,

causing the deviation from the linear Stern-volmer plots. However, in our work, this is not an accountable reason for the downward curvature at stern-volmer relationship when the ruthenium complex concentration is low since the plots did show severe downward tendency when the concentrations is around or lower than 2.81 mM. Uniform distribution of ruthenium complex at low concentration is expected due to the hydrophilic property of PEG-DA matrix and this was further confirmed by the confocal brightfield image of the PEG hydrogel with encapsulated ruthenium complex at low concentration shown by other researchers[14]. However, ruthenium complex cluster still should be considered when the ruthenium complex concentration is very high since the excess amount of ruthenium complex in PEG-DA membrane will lead to the cluster of fluorescent dyes. Too many ruthenium complex entrapped in PEG-DA matrix will force dyes to aggregate together and form a cluster with larger size which is hard to be washed away from the network of hydrogel. Thus, the downward curving of the line representing higher ruthenium concentration will be strengthened and will not be considered as a suitable concentration used for sensor fabrication.

As shown in the plot of relative sensitivity vs. ruthenium concentrations in Fig. 5(b), sensitivity is increased with increasing amounts of immobilized fluorophore at room temperature under atmospheric pressure. However, the relative sensitivity reaches a maximum at a ruthenium loading of 2.81 mM, which implies that this amount is considered to be the limit that can be effectively incorporated in the PEG-DA membrane. Combined with the results from Fig. 5(a), a concentration of 2.81 mM was found to be the optimum one for later experiment since ruthenium complex at this concentration can disperse uniformly in the PEG-DA matrix and yield the highest relative sensitivity.

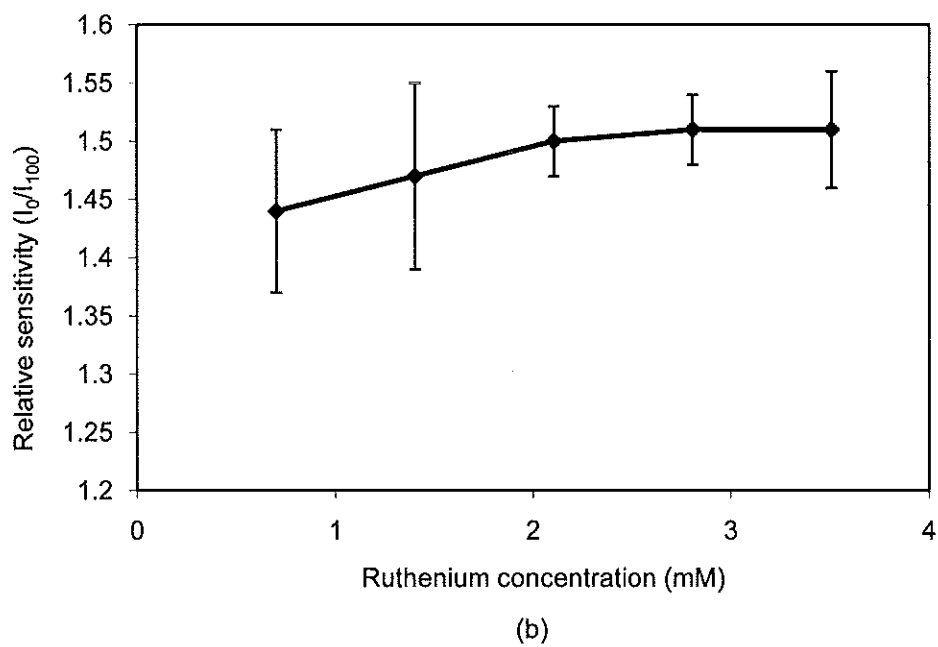
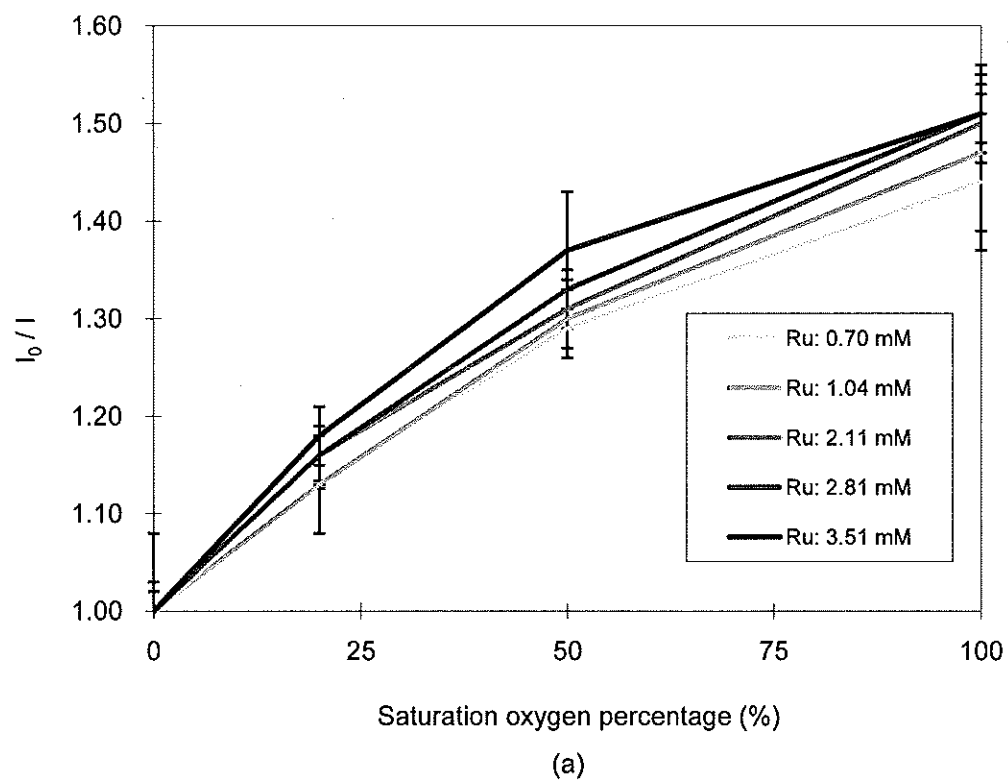


Fig. 5. Optical properties of oxygen sensitive PEG-DA membranes on SU-8 surface.

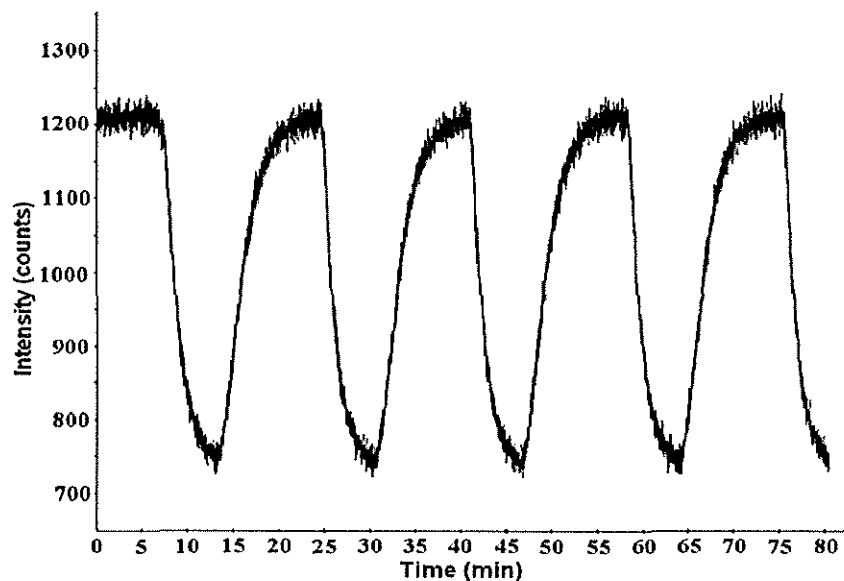
As shown in figure, 5. (a) is Stern-Volmer plots for materials comprised of various ruthenium concentrations in PEG-DA membranes, and 5. (b) is Relative sensitivity ( $I_0/I_{100}$ ) as a function of ruthenium complex concentration in PEG-DA membrane.

### 3.5 Response time and reversibility

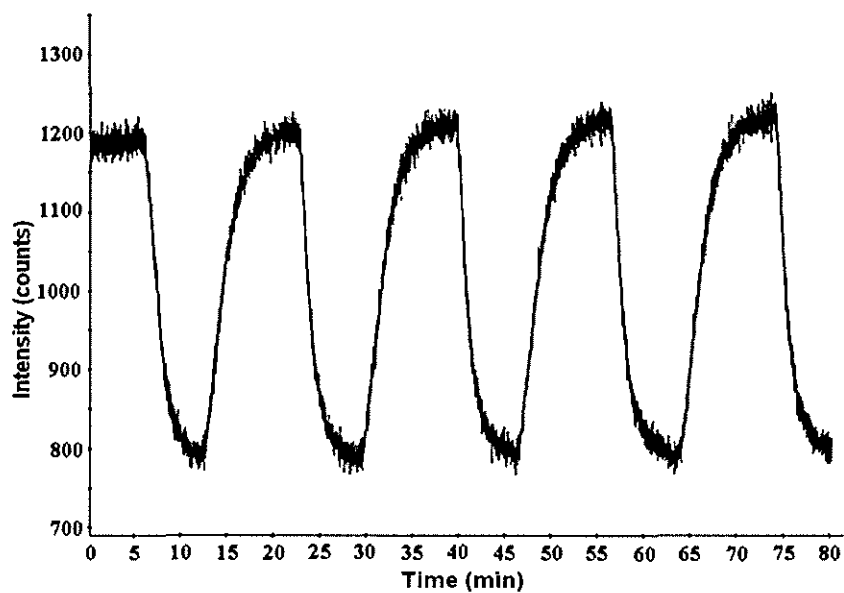
The response time and reversibility of the oxygen sensitive membrane with optimal ruthenium complex concentration of 2.81mM was tested by alternating saturation oxygen percentage. Before conducting the measurement, the sensor was immersed in D.I. water for 12 hours and expose to the LED light source. This step was done to remove any possible excess ruthenium dyes and unreacted PEG-DA monomers as well as to avoid any initial instability as mentioned in Section 3.3. As shown in Fig. 6(a), the signal changes were fully reversible, and the response time was consistent. This result demonstrates the sensor to be highly reproducible with an excellent reversible response to dissolved oxygen in water and these indicate that the PEG-DA is a good candidate for optical sensor application. First of all, the fluorophore entrapped in PEG-DA membrane did not leach out during measurement since every time the highest intensity was measured when there is 90% of saturated oxygen concentration. No sign of deterioration appear when the sensing elements exposed to the LED since the fluorescence intensity at certain dissolved oxygen concentration is reversible. Both of them demonstrate that PED-DA is a qualified optical oxygen sensor matrix material.

Fig. 6(a) also shows the typical response curve of the ruthenium complex. The response time from nitrogen to oxygen saturated D.I. water was about 5 minutes (90% response from 0% to 100% oxygen), whereas the shift from oxygen to nitrogen saturated water took about 10 minutes (90% response from 100% to 0% oxygen). The response time is slow but it can be improved after analyzing the reasons underlying. The response time consists of two parts. One is the amount of time it took for dissolution of oxygen into D.I. water, which is dependent on the gas bubbling rate and water volume. Slow gas bubbling rate and large water volume (20 ml) prolong the response time. Better response time can be expected since the only small amount water needed if we integrate the sensing elements within microfluidic channels. The other one is the amount of time

needed for oxygen molecules being transferred into the PEG-DA hydrogel cross-linked network. The time is limited by the diffusion rate of oxygen molecule which is close related to the shape and structure of hydrogel matrix. Increasing the ratio of surface area-to-volume will lead to the fast response time. Several methods can be applied to increase the ratio of surface area-to-volume of matrix: minimizing the pattern size, increasing the mesh size, fabricating thinner matrix. All of them are feasible and easy manipulations for PEG-DA matrix. However, some drawbacks will be brought at the same time. For instance, although increasing the mesh size of hydrogel will enhance the diffusion rate of oxygen molecules, it will be followed by the leaching of dyes. Although it takes less time for oxygen molecule to diffuse in thin PEG-DA matrix, less fluorescent intensity can be detected since less ruthenium complex is entrapped in the thin PEG-DA matrix. Considering the goal of this work is to develop a simplified sensor model used to test the feasibility of our chemically anchoring technique for PEG-DA matrix on SU-8 surface, it is not necessary to acquire optimum response time here.



(a)



(b)

Fig. 6. Response time and reversibility of fluorescence intensity changes of PEG-DA membrane upon switching between nitrogen and oxygen saturated D.I. water repeatedly. (a) The sample stored in D.I. wafer for 1 day (b) The sample stored in D.I. water for 2 months.

A follow-up study was completed after storing the PEG-DA matrix to in D.I. water for a period of two months. The response time and reversibility of the stored simplified sensor were investigated again. Fig. 6(b) shows a good reversibility on a typical response curve with the similar response time. No delamination or degradation of PEG-DA membrane appeared during the whole process. Therefore, the PEG-DA matrix has successfully been used to entrap the ruthenium complex and it was covalently bound to SU-8 surface through our simple photoinitiation steps.

### 3.6 Long-term storage stability

Every fifteen days, this simplified fluorescent oxygen sensor was taken out from the D.I. water storage container and subjected to fluorescent measurements. The data in Fig. 7 demonstrate that the simplified sensor is stable within the error of the laboratory test system and exhibits good long-term stability when ruthenium complex was physically incorporated in a PEG-DA matrix covalently bond on SU-8 for two months. No noticeable physical shape change of the matrix or delamination of PEG-DA matrix from the SU-8 surface was observed after two months storage. It indicates that our photoinduced chemically anchoring technique can be used to covalent bond the thick PEG-DA matrix to SU-8 successfully and does not exhibits any negative effects on the structure of matrix.

Though the shape and the chemical bonding of matrix remain the same, the relative sensitivity of the simplified sensor decreased 5% from the original sensitivity during the two months period. This phenomenon is caused by the photobleaching of ruthenium complex. This explanation seems to be contradictive with the stable state of fluorophore after initial stability step and the measurement results during the reversibility testing since they were used as evident that instinct characteristic of fluorophore is not the main reason for the fluorescent intensity decrease. It is true that photobleaching of fluorophore has small effects at that two stages, however, this does not mean that it has no effect for the overall relative sensitivity of the simplified sensor after a long period. Since PEG-DA matrix with the same molecular weight, 575 and similar components used in our work was reported to hinder the fluorophore from leaching very well,

photobleaching was considered to be the main reason for the intensity decrease for long-term storage.

This effect of photobleaching can be minimized by measuring the lifetime of the fluorophore,  $\tau$  or the corresponding phase shift,  $\Phi$ , virtually independent of external perturbations. According to the work done by other groups with these time-resolved measurements, the relative sensitivity of optical oxygen sensor decreased about 5% over 12 months [19]. However, the long-term storage stability data is still impressive since the measurement is based on the intensity rather than lifetime or phase shift. Better long-term storage result can be expected if the lifetime or phase shift of ruthenium complex entrapped in PEG-DA matrix was measured.

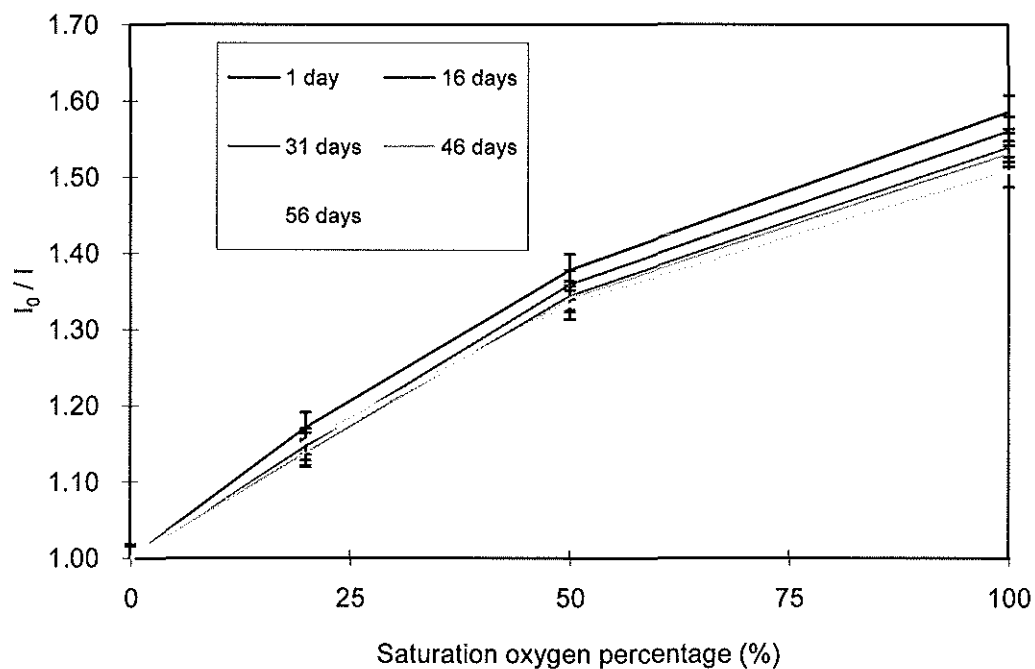
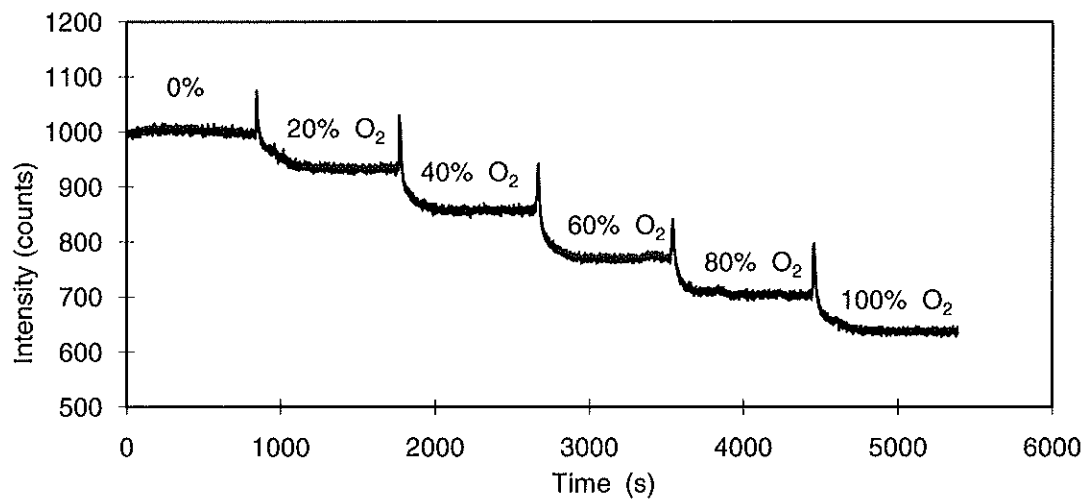


Fig. 7. Long-term stability of ruthenium complex incorporated in chemically anchored PEG-DA membrane on SU-8 surface.

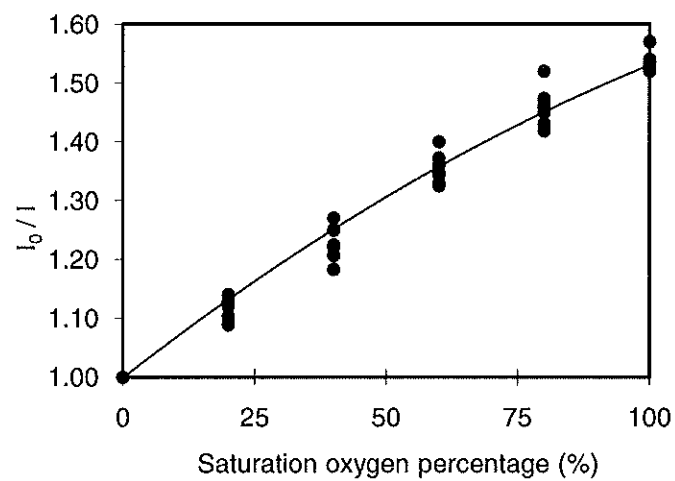
### 3.7 Dissolved oxygen measurements within SU-8 channel

Three sealed SU-8 channels with patterned optical oxygen sensitive membrane embedded were fabricated and tested by sequentially injecting a series of D.I. water with difference dissolved oxygen concentrations. Prior to the experiments, the SU-8 channel was first filled with N<sub>2</sub>-saturated D.I. water for 30 minutes to ensure the fluorescent intensity of oxygen sensitive membrane is maximal. After this, testing solution was injected into the SU-8 channel sequentially and each time more dissolved oxygen was added. During the oxygen measurement, 10 ml D. I. water was saturated by bubbling N<sub>2</sub> gas and O<sub>2</sub> gas at different ratio in a separate glass container for 15 minutes. After saturation step, the testing solution was transferred with a 5 ml syringe and injected into the SU-8 channel. Immediately after injecting each solution, the distal ends of plastic tubing at inlet and outlet ports were capped with fittings to minimize the influence of ambient air. As shown in Fig. 8(a), the fluorescent intensity at the emission wavelength, 608 nm, decreased with the increase of the dissolved oxygen content. At each oxygen content, six fluorescent intensity points were recorded randomly when the signal tends to be stable. The Stern-Volmer relationship plotted in Fig. 8(b) based on these data, which is a common method to evaluate the optical oxygen, show a similar non-linearity tendency described in previous oxygen measurements for the oxygen assembly system in section 3.3.4. All these results indicate that the optical oxygen sensitive membrane remains its sensitivity even if it was integrated within sealed SU-8 channel.

During the initial stability step and the oxygen concentration experiment, cylindrical hydrogel structure remained in the middle of the SU-8 channel without physical shape change and migrating. This clearly demonstrates that PEG-rich hydrogel was covalently immobilized on planar SU-8 surface within sealed fluidic channel by simply utilizing our novel surface modification technique. Potential of this technique is anticipated since it can be applied after channel bonding process. Feasibility of integration of bioanalytical elements or polymer films, which is sensitive to harsh environment required for bonding process, is enhanced.



(a)



(b)

Fig. 8. Dissolved oxygen measurements for cylindrical PEG-based sensing structure chemically anchored after bonding process.

As shown in Figure, 8. (a) is typical time response of optical fluidic sensor with different oxygen concentrations, and 8. (b) is relative sensitivity ( $I_0 / I$ ) as a function of saturation oxygen percentage in PEG-DA membrane embedded in SU-8 fluidic channel.

#### 4. CONCLUSIONS

Surface bound PEG-rich hydrogel matrix containing an oxygen-sensitive fluorophore were synthesized for potential application in fluidic channels that utilize photoresist SU-8 as structure material. The PEG-DA matrix was chemically anchored to the SU-8 surface through the use of a surface-bound photoinitiator which acted as a site for chain growth. These densely crosslinked polymeric networks were suitable structures for the physical entrapment of the oxygen-sensitive ruthenium complex with significant fluorophore leaching occurring only in the initial washing steps. The reported hydrogel matrix exhibited fluorescence quenching behavior with Stern-volmer relationship. Long-term storage stability and reversibility were also successfully demonstrated, illustrating that this surface bound PEG-rich matrix is a good candidate for the immobilization of fluorophores for a long-term use.

An optical oxygen fluidic channel sensor was fabricated and integrated with PEG-rich matrix after bonding process by utilizing our novel surface modification technique. Good performance of dissolved oxygen content measurement was demonstrated and no physical shape change and immigrating of PEG-rich hydrogel within channel was detected. To my knowledge, it is the first time to report the method which can be used to integrate the PEG-based hydrogel structure after channel bonding process within a polymeric channel structure. This merit enhances the potential applications of PEG-based hydrogel as matrix material for integrated BioMEMS since bioanalytical elements are easy to lose its activity when temperature or pressure required for bonding is too high.

#### ACKNOWLEDGEMENTS

This work was partly supported by a grant from NIH (EB006611-01).

## REFERENCES

- [1] G. M. Whitesides, "The origins and the future of microfluidic," *Nature*, 442, 2006, pp. 368-373.
- [2] X. L. Xiong, D. Xiao, M. M. F. Choi, "Dissolved oxygen sensor based on fluorescence quenching of oxygen-sensitive ruthenium complex immobilized on silica-Ni-P composite coating," *Sens. Actuators B*, 117, 2006, pp. 172-176.
- [3] A. Mills, "Optical oxygen sensors: utilizing the luminescence of platinum metals complexes," *Platinum Met. Rev.*, 41, 1997, pp. 115-127.
- [4] H. Lorenz, M. Despont, N. Fahmi, N.L. Bianca, P. Renaud, M.J. Vettiger, "SU-8: a low cost negative resist for MEMS," *J. Micromech. Microeng.*, 7, 1997, pp. 121-124.
- [5] P. Abgrall, V. Conedera, H. Camon, A.M. Gue, N.T. Nguyen, "SU-8 as a structural material for labs-on-chips and microelectromechanical system," *Electrophoresis*, 28, 2007, pp. 4539-4551.
- [6] G. Kotzar, M. Freas, P. Abel, A. Fleischman, S. Roy, C. Zorman, J. M. Moran, and J. Melzak, "Evaluation of MEMS materials of construction for implantable medical devices," *Biomaterials*, 23, 2002, pp. 2737-2750.
- [7] J. Steigert, O. Brett, C. Müller, M. Strasser, N. Wangler, H. Reinecke, M. Daub, and R. Zengerle, "A versatile and flexible low-temperature full-wafer bonding process of monolithic 3D microfluidic structures in SU-8," *J. Micromech. Microeng.*, 18, 2008, 095013 (8pp).
- [8] S. Li, C. B. Freidhoff, R. M. Young, R. Ghodssi, "Fabrication of micronozzles using low-temperature wafer-level bonding with SU-8," *J. Micromech. Microeng.*, 13, 2003, pp. 732-738.
- [9] C. Pang, Z. Zhao, L. D. Du, Z. Fang, "Adhesive bonding with SU-8 in a vacuum for capacitive pressure sensors," *Sens. Actuators, A*, 147, 2008, pp. 672-676.
- [10] Otto S. Wolfbeis, "Materials for fluorescence-based optical chemical sensors," *J. of Mater. Chem.*, 15, 2005, pp. 2657-2669.
- [11] *Hydrogel in medicine and pharmacy*, vol. 1, 1st ed., CRC Press Inc., Boca Raton, Florida, 1986, pp. 96.
- [12] D.P. O' Neal, M.A. Meledeo, J.R. Davis, B.L. Ibey, V.A. Gant, M.V. Pishko, G.L. Coté, "Oxygen sensor based on the fluorescence quenching of a ruthenium complex immobilized in a biocompatible poly(ethylene glycol) hydrogel," *IEEE Sens. J.*, 4, 2004, pp. 728-734.
- [13] S. Lee, B. L. Ibey, G. L. Coté, M. V. Pishko, "Measurement of pH and dissolved oxygen within cell culture media using a hydrogel microarray sensor," *Sens. Actuators B*, 128, 2008, pp. 388-398.
- [14] R. J. Russell, A.C. Axel, K.L. Shields, M.V. Pishko, "Mass transfer in rapidly photopolymerized poly(ethylene glycol) hydrogels used for chemical sensing," *Polymer*, 42, 2001, pp. 4893-4901.
- [15] Y.L. Wang, M. Bachman, C.E. Sims, G.P. Li, N.L. Allbritton, "Simple photografting method to chemically modify and micropattern the surface of SU-8 photoresist," *Langmuir*, 22, 2006, pp. 2719-2725.
- [16] Y.L. Wang, J.H. Pai, H.H. Lai, C. E. Sims, M. Bachman, G.P. Li, N.L. Allbritton, "Surface graft polymerization of SU-8 for bio-MEMS application," *J. Micromech. Microeng.*, 17, 2007, pp. 1371-1380.

- [17] S. L. Tao, K.C. Popat, J. J. Norman, T. A. Desai, "Surface modification of SU-8 for enhanced biofunctionality and nonfouling properties," *Langmuir*, 24, 2008, pp. 2631-2636.
- [18] Z.Gao, D.B. Henthorn, C.S. Kim, "Enhanced wettability of an SU-8 photoresist through a photografting procedure for bioanalytical device applications," *J. Micromech. Microeng.*, 18, 2008, 045013 (7pp).
- [19] C. McDonagh, C. Kolle, A. K. McEvoy, D. L. Dowling, A. A. Cafolla, S. J. Cullen, B. D. MacCraith, "Phase fluorometric dissolved oxygen sensor," *Sens. Actuators B*, 74, 2001, pp. 124-130.

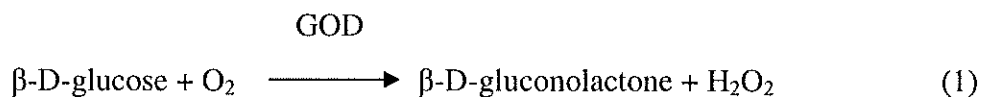
### III. A dry film fluorescence glucose microfluidic sensor with in-device PEG-based sensing element

#### ABSTRACT

A novel transparent dry film resist (DFR), PerMX 3000 series, was utilized as main structure material to fabricate a fluorescent enzyme-based microfluidic glucose sensor. This sensor was based on the enzymatic reaction of glucose oxidase (GOD) that catalyzes the oxidation of glucose. Ruthenium complex fluorophore was adapted as a reporting agent due to its quenching behavior by oxygen molecules. Both the oxygen-sensitive ruthenium complex and GOD were incorporated into poly (ethylene glycol) (PEG)-based hydrogel materials, which were lithographically patterned and embedded inside PerMX microfluidic channel after bonding process. A linear range from 0 to 10 mM (0 to 180mg/dl) glucose with good sensitivity was demonstrated with optimal enzyme concentration of 0.033 mM/ml PEGDA repeatedly (n=9) in our study. Good reversibility and repeatability was observed. This finding also demonstrates the promise of the PerMX microfluidic systems as platforms for various enzyme-based optical assays.

#### 1. INTRODUCTION

Glucose sensors that utilize glucose oxidase (GOD) as the recognition element have been studied extensively recently. GOD is highly selective for  $\beta$ -D-glucose and catalyzes its oxidation according to:



The detection of oxygen consumption due to the enzymatic reaction has been widely applied as an indirect indication of glucose concentrations [1]. One promising approach for oxygen detection is to take advantage of the quenching behavior of molecular oxygen toward certain fluorophores [2]. Compared with conventional electrochemical glucose sensors; fluorescence glucose sensors based on fluorophores

possess certain merits- for instance, there are no requirements for electrodes and no electromagnetic interference [3, 4].

A variety of oxygen-dependent fluorescence glucose sensors have been developed and investigated recently. Otto et al. reported planar glucose sensors with entrapped GOD in a sol-gel film doped with the oxygen-sensitive fluorophore, ruthenium (II) (4, 7-diphenyl-1, 10-phenanthroline)<sub>3</sub>-(dodecylsulfate)<sub>2</sub> (Ru(dpp)) [5]. The McShane group employed the polyelectrolyte-coated calcium alginate microspheres to encapsulate GOD and an oxygen-quenched fluorophore to form a spherical fluorescent sensor system [6]. Moreno-Bondi et al. developed an optical glucose fiber sensor with the sensing layer coating at the tip of the optical fiber [7]. But, few applications of integrating enzyme and oxygen-sensitive fluorophore within microfabricated channel systems have been reported. Since the microfluidic channel systems promise the potential to create portable miniaturized instruments, it is of interest to utilize them as platforms for fluorescence enzyme-based glucose sensors.

To date, the common main structural materials of microfluidic channels in micro-total analysis system for biological analysis are polymeric materials, such as poly (dimethylsiloxane), or the epoxy-based photoresist SU-8, because they can be applied to fabricate fully monolithic microfluidic system with uniform surface properties at reduced cost [8]. However, the hydrophobic nature of these materials has posed several issues [9, 10]. It is hard to fill solutions into hydrophobic microfluidic channel without external force and it is easy to encounter nonspecific protein adsorption if the sensor is to come in contact with physiological fluids. Surface modification has become indispensable to enhance the wettability inside the microfluidic channel and to minimize biofouling, which increases fabrication complexity. Moreover, SU-8 photoresist also presents a limitation about layer stacking with high intrinsic shrinkage after the post-exposure baking step [11]. A good seal of the microfluidic channel is hard to be achieved if ultra-thick polymer to polymer layers are required. Recently, dry film resists (DFRs) have been investigated as potential materials in the fabrication of microfluidic devices [12]. Originally developed for printed circuit board and wafer level packaging, DFRs possess many advantages, including excellent adhesion to silicon and glass substrate, good planarity of stacked films, short processing time, and near-vertical side wall formation.

In our work, PerMX 3000 series, a novel epoxy-based negative-tone DFR developed by DuPont Company was introduced and utilized as the main structural material for monolithic microfluidic channels. It is optically transparent and more wettable than conventional epoxy-based photoresists such as SU-8 photoresist. Poly (ethylene glycol) diacrylate (PEGDA), a widely-used photopatternable macromonomer, was utilized as the matrix material for the immobilized sensing element. To avoid exposure of the enzyme to the relative high temperatures ( $>65^{\circ}\text{C}$ ) utilized during the bonding process, GOD was chemically immobilized in the PEG-rich hydrogel sensing element after completion of the microfluidic channel [13]. Feasibility of this approach had already been demonstrated in our previous work [14]. The fabricated devices were then used to measure glucose concentrations to demonstrate the potential application of PerMX DFR in the construction of enzyme-based microfluidic biosensors.

## **2. EXPERIMENTAL**

### **2.1 Materials**

Glucose oxidase (from *Aspergillus niger*), poly (ethylene glycol) diacrylate with an average molecular weight of 575, HCPK photoinitiator, the oxygen sensitive fluorescent compound ruthenium complex, dichlorotris (1, 10-phenanthroline) ruthenium (II) hydrated 98%, toluene, acryloyl chloride were purchased from Sigma-Aldrich (St. Louis, MO). Acetone, methanol, isopropanol, and sodium carbonate were obtained from Fisher Scientific (Fair lawn, NJ). SU-8 developer (PGMEA) was obtained from MicroChem (Newton, MA). Liquid photoinitiator, DAROCUR 1173 was purchased from Ciba specialty chemicals company (Berwick, PA). PerMX 3000 series DFR was received from Dupont Company (Wilmington, DE).

## 2.2 Glucose oxidase (GOD) activation

GOD was activated by acryloyl chloride in Falcon™ six well flat bottom plates from Becton Dickinson Labware (Franklin Lake, NJ). Sodium carbonate buffer was freshly prepared by dissolving 300 mg sodium carbonate in 5 ml D. I. water. The precursor solution including 0.01 g glucose oxidase, 5 ml sodium carbonate and 2 μl acryloyl chloride were added into 6 well plates and remained at 4 °C in refrigerator for 5 hours because acryloyl chloride reacts vigorously. The underlying principle of the reaction is shown in Figure 1. The surface amino groups of GOD were reacted with acryloyl chloride and generated activated GOD with surface methacrylate groups. After the reaction, the enzyme solution was pipetted and filled into the dialysis tubing from Fisher Scientific (Fair Lawn, NJ) for 12 hours purification. Purified activated GOD solution was pipetted out of the dialysis tubing and stored in a glass bottle at 4 °C for further use.

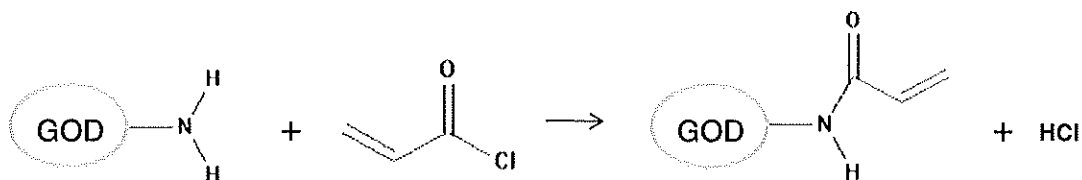


Figure 1 The functional modification of glucose oxidase by acryloyl chloride.

## 2.3 Dry film channel fabrication

PerMX DFR with 50 μm thickness was cut into 25 cm by 50 cm rectangular pieces. A glass slide used as cover layer was cleaned in acetone, methanol and D.I. water for 3 minutes and dried in air for 30 seconds respectively. Inlet and outlet holes were drilled before the lamination step. Then, the glass slide was placed on a hotplate at 200 °C for 15 minutes of dehydration. After the dehydration step, the cleaned glass slide was placed in the chamber of a reactive ion etching system (PE-200, Plasma Etch). Oxygen plasma treatment was applied to remove organic residue and to improve the PerMX DFR

adhesion to glass substrate. PerMX DFR adhesion was further enhanced through a post-lamination baking at 95 °C for 4 minutes and a hot roll lamination process with thermal lamination instrument (TL901, 3M Stationery Products Division).

The details of the PerMX DFR channel bonding process are described in Figure 2. Inlet and outlet ports (Figure 2(a)) were patterned in alignment with the inlet and outlet holes using mask #1 and a mask aligner instrument (Karl Suss MA6, Suss MicroTech). The intensity of UV light source with wavelength at 365 nm is 5.7 mW/cm<sup>2</sup> during the whole channel fabrication process and the total exposure energy used for the first DFR layer was 675 mJ/cm<sup>2</sup>. Then, the first dry film layer was cured by placing on a hotplate at 95 °C for 4 minutes in the post-exposure baking step, with the polyethylene layer peeled off after the glass slide had cooled to room temperature. The second and third layers of PerMX DFR were laminated on the first one directly through a hot rolling process. The cover layer was aligned with mask #2 and exposed to UV light again to pattern the fluidic channel structure. PerMX DFR channel structure was completely cured after 8 minutes at post-exposure baking step and developed after soaking in PGMEA for 9 minutes. All the uncured DFR residues were cleaned by utilizing isopropanol.

The bottom layer was cleaned using the same procedure and treated with oxygen and argon plasma. In the center of the cleaned glass slide, a 50 µm thick piece of PerMX DFR was laminated and baked on a hotplate at 95 °C for 4 minutes, then cooled to 65 °C for 4 minutes to anneal the small cracks on the uncured DFR surface caused by peeling off the polyester coversheet film. In order to obtain tight contact between the cover layer and the bottom layer, bonding process was conducted with an external pressure at 65 °C for 1 minute. Finally, the completed cured PerMX DFR channel was achieved through a flood UV exposure and a post exposure bake at 95 °C for 4 minutes.

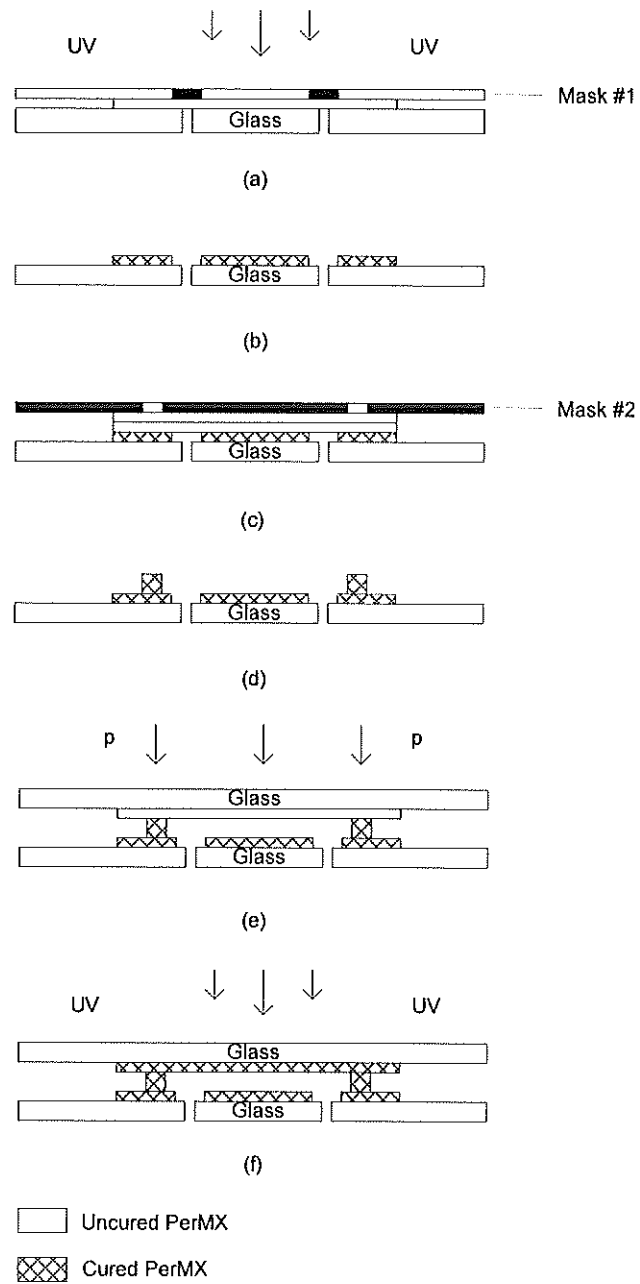


Figure 2 Bonding procedure of PerMX fluidic channel structure.

## 2.4 Integration of glucose sensing elements

PEGDA monomer solution of 5 ml was mixed with 2 ml activated GOD solution ( $\text{pH}=7.42 \pm 0.1$ ) in a brown glass bottle at room temperature. Ruthenium complex of various concentrations and 100 mg liquid initiator, DAROCUR 1173, were added. The mixture was then stirred with magnetic stirrer for 1 hour to obtain homogenous distribution of fluorophore and enzyme. Then, nitrogen gas was bubbled into mixed solution for 30 minute to remove oxygen molecules, a typical inhibitor for photoinduced polymerization reactions. Immediately after this, the freshly mixed solution was injected into the bonded PerMX DFR channel and the ends of inlet and outlet tubing were capped to form an oxygen-free environment. The bottom of fluidic channel placed with a mask #3 was exposed to UV light ( $5.7 \text{ mw/cm}^2$ , 365nm, 2 minutes) to form a cylindrical PEG-based optical glucose sensing structure within the sealed channel. Unpolymerized solution was rinsed out of channel by injecting standard buffer solution repeatedly after exposure step. In this PEG- based hydrogel structure (as shown in Figure 3), activated GOD was covalently immobilized through the free radical reaction while ruthenium complex was physically entrapped due to the densely crosslinked network.

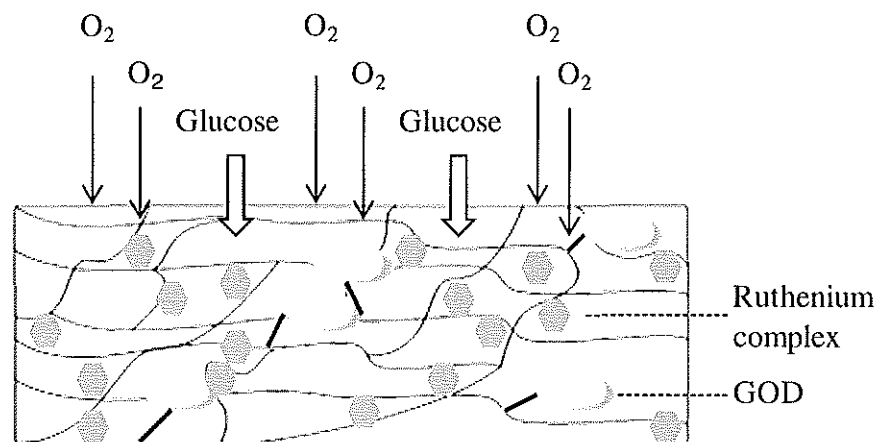


Figure 3 Cross-sectional diagram of PEG-based hydrogel with entrapped ruthenium complex and immobilized GOD.

After the whole fabrication process, the integrated optical DFR fluidic channel was filled with standard buffer solution and exposed to LED light source for 12 hours to test initial stability before glucose measurements were conducted.

## 2.5 Device design

As shown in Figure 4 (a), an oval-shape chamber was built in the middle of the microfluidic channel. This chamber served as a detection chamber where enzyme-based glucose reaction and fluorescence detection occurred. In our study, this detection chamber was designed for easy alignment of photomask. In order to avoid the harsh conditions during the bonding process, the sensing element was patterned inside PerMX channel after bonding process. The size of PEG-based sensing element was larger than the designed size due to the refraction of UV light going through the glass substrate and PerMX layer. Obviously, careless alignment of photomask was possible to make it difficult to confine sensing element in the center part of chamber and thus, tended to block one side of channel. So, in this study, central detection chamber with widest part of 5 mm was designed and applied. The details of enlarged top view of this part are presented in Figure 4 (c).

Another important part of this microfluidic system was the importation (exportation) part. A circle pattern was made on top of inlet and outlet holes to prevent layer edge delamination from glass substrate, which always happened if holes were punched directly on the crosslinked PerMX layer. The circle pattern was created on the bottom layer of PerMX with diameter of 4 mm (As shown in Figure 4 (b)), larger than the diameter of inlet and outlet holes on the glass slides. And the top view of real channel structure is shown in Figure 4 (d).

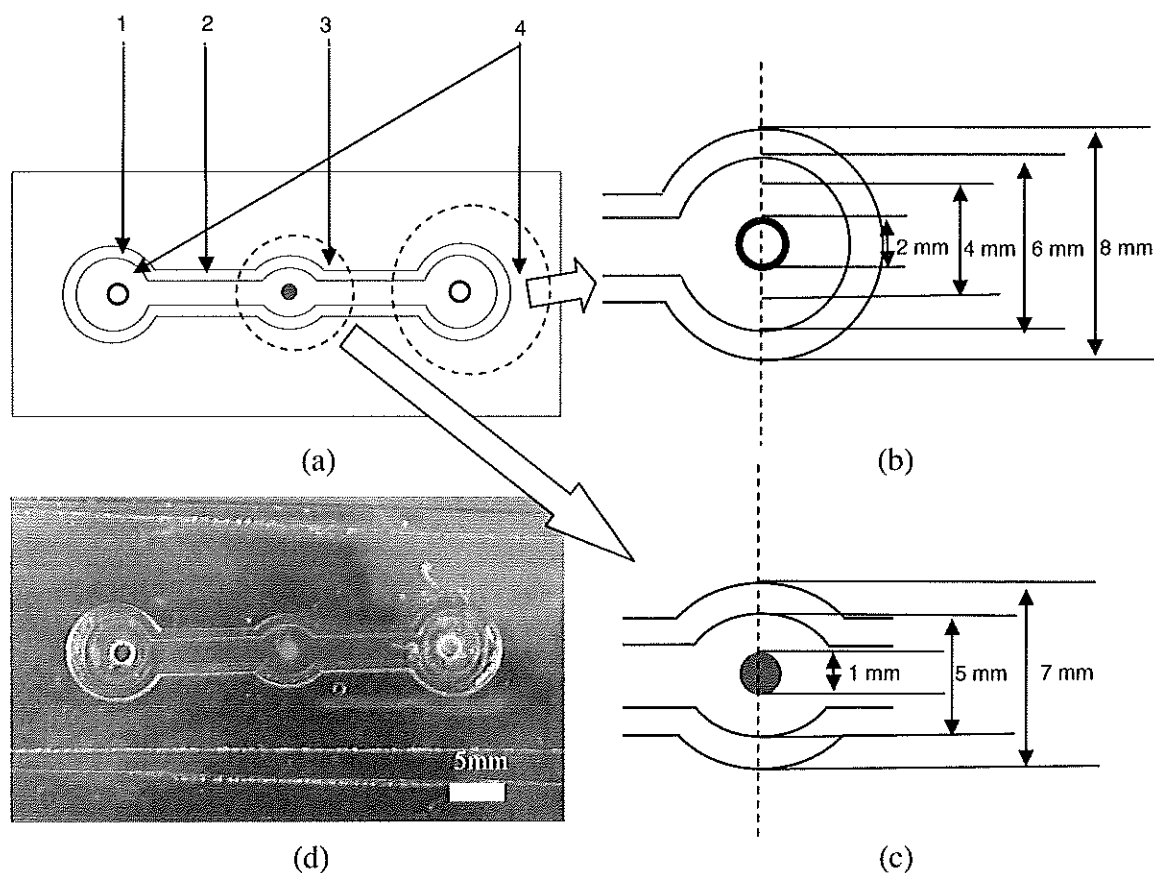


Figure 4 Top view diagrams and photography of integrated fluorescent glucose microfluidic channel.

As shown in figure, 4(a) is the top view diagram of microfluidic channel: 1. PerMX channel wall structure; 2. Sealed monolithic PerMX microfluidic channel; 3. PEG-based sensing element; 4. Inlet and outlet holes on glass substrate. 4(b) is the enlarged details of the inlet (outlet) holes of the channel, 4(c) is the enlarged details of the detection chamber of the channel, 4(d) is photography of the bonded microfluidic channel integrated with PEG-based sensing element.

## 2.6 Instrumentation

The measurement setup for glucose detection is depicted in Figure 5. All fluorescence intensity measurements were operated with a spectrofluorometer (USB2000-FLG, Ocean Optics) and data were collected using SpectraSuite software. A blue LED (LS450, Ocean Optics) was used as the excitation light source and the excitation and emission wavelengths of ruthenium complex were 470 nm and 608 nm respectively. The blue light source was connected to the spectrometer by using a reflection probe (R200-7-UV-VIS, Ocean Optics) with six illumination fibers (200  $\mu\text{m}$  diameter each) and one reading fiber (200  $\mu\text{m}$  diameter) in the center of the probe. A high-pass filter ( $>540\text{nm}$ ) was set to eliminate the excitation light affecting the spectrometer. All the glucose measurements were taken in a dark environment to minimize any stray light effects.

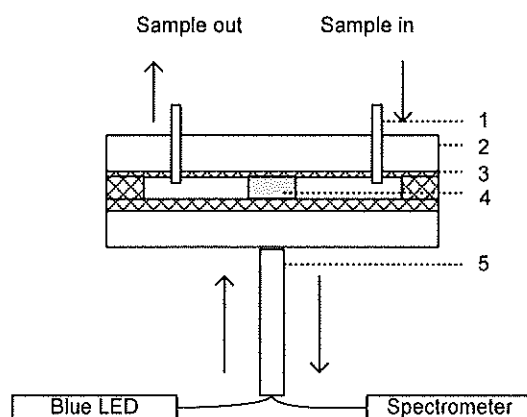


Figure 5 Measurement setup for optical glucose PerMX DFR fluidic channel sensor.

- (1) Fluorinated ethylene propylene tubing.
- (2) Glass slide.
- (3) Cured PerMX.
- (4) PEG-based hydrogel.
- (5) Reflection probe.

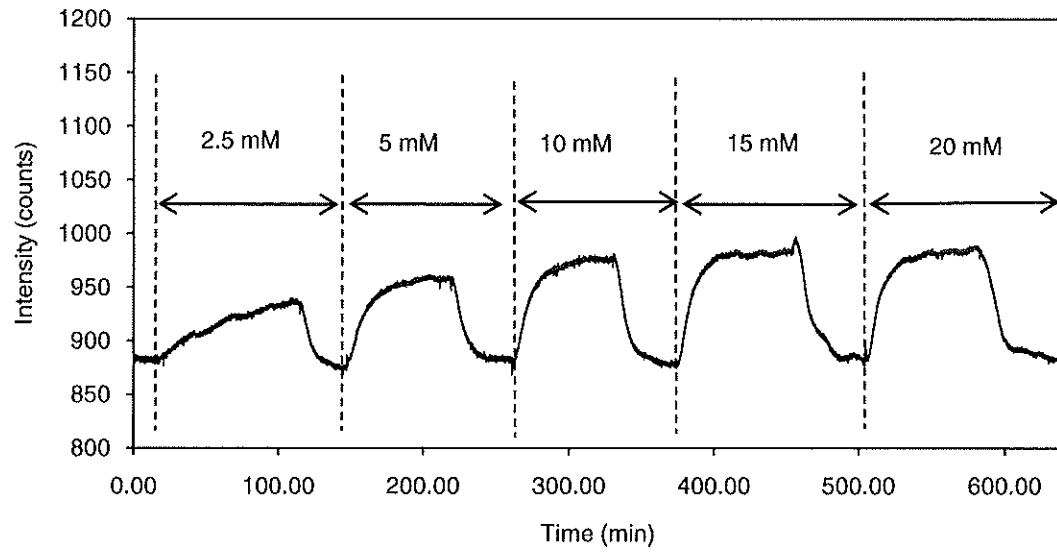
All phosphate buffer solution (PBS) of  $\text{pH } 7.42 \pm 0.1$  at  $20\text{ }^\circ\text{C}$  were prepared by dissolving the buffer salt (Fisher Scientific, NJ) into D.I. water. Glucose testing solution was prepared with PBS. Before glucose measurements, the standard buffer solution and glucose working solution were equilibrated with air. Freshly prepared standard buffer or glucose testing solution was injected into the PerMX fluidic channel by using a 5 ml syringe alternatively. When the optical glucose fluidic sensor was not in use, it was filled with PBS and stored at  $4\text{ }^\circ\text{C}$  in the refrigerator.

### **3. RESULTS AND DISCUSSIONS**

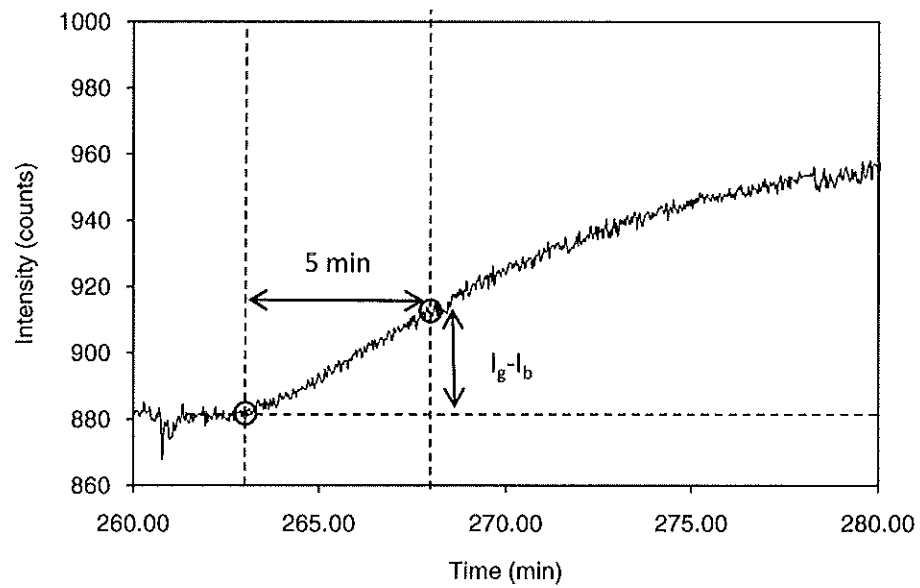
#### **3.1 Typical time response**

Our design utilized the measurement of oxygen to indirectly monitor glucose concentrations. During the enzymatic reaction, glucose was oxidized in the presence of oxygen to  $\beta$ -D-gluconolactone, with a byproduct of the reaction being hydrogen peroxide (see Equation 1). Optical monitoring of glucose concentrations could be achieved by detecting the consumption of oxygen in the microenvironment of the sensing element. In this work, we utilized the oxygen quenching behavior attributed to the ruthenium complex to monitor the glucose reaction. From the experiment point of view, the optical intensity reflects the local oxygen concentration in the sensor element area. Since the fluorescence of the ruthenium complex was quenched in the presence of oxygen, increasing fluorescence signal resulted from the consumption of molecular oxygen and was correlated with increased glucose concentrations.

Response curves of the glucose biosensor subjected to various glucose concentrations (2.5 mM, 5 mM, 10 mM, 15mM and 20 mM) were recorded using the SpectraSuite software and displayed in Figure 6. Since the volume of the glucose testing solution in the fluidic channel was much larger than the volume of the PEG-based sensing element, bulk oxygen and glucose concentrations were considered to be constant during glucose measurement. Thus, the changes of fluorescence intensity were due to the local oxygen change inside the sensing element rather than the oxygen depletion in the bulk solution.



(a)



(b)

Figure 6 Typical response curves for glucose measurements.

(a) Response curve at various glucose concentrations,

(b) Enlarged view of the initial response curve at glucose concentration of 10 mM.

During the storage period or initial stabilization step, microfluidic channel shown in Figure 4 was always filled with PBS at a state of air-saturation. Thus, local oxygen concentration inside element remained at 0.26 mM at the beginning of glucose measurement (dissolved oxygen concentration for air-saturated solution at 20 °C). As shown in Figure 6(a), fluorescent intensity remained constant before glucose introduction. When the sensor started to be filled with glucose solution, sensor response (fluorescent intensity) increased. This was attributed to dissolved oxygen inside PEG-based sensing element being consumed during enzyme reaction. Gradually, the local oxygen consumption rate became slower since less oxygen molecules remained inside sensing element, while the oxygen diffusion rate (oxygen replenishment rate) became faster due to higher oxygen gradient. At some point in time, the oxygen consumption rate would be balanced with oxygen diffusion rate, and the system was said to be at steady state. At steady state, local oxygen concentration and fluorescence intensity would remain unchanged. Once sensor response was stabilized, PBS in a state of air-saturation would be injected into channel again to calibrate intensity signal back to baseline and make it ready for next measurement.

### **3.2 Calibration curve for glucose measurement**

Normally, glucose concentration was measured through obtaining maximum fluorescent intensity at steady state. However, in our work, the time required to reach steady state was incompatible with its use as a device for dissolved glucose monitoring. Our device instead utilizes a differential method, where the initial rate of reaction was measured, since the reaction occurred sufficiently slowly [15, 16]. Using this method, local oxygen change rates (slopes) were measured at the initial stage of glucose reactions (the linear range of response curve). Figure 6 (b) was the enlarged views of response curve at a glucose concentration of 10 mM. As shown in this figure, response curve was linear during 5 minutes at early stage of enzyme reaction. Based on the definition of slope, within this 5 minutes period, slope was equal to the intensity change rate. However, for each microfluidic channel, the fluorescent intensity at baseline was not exactly the same. A slight change of detection probe setup, such as the illumination part of sensing element at sensing element, the position and tilted angle of probe, would result in different

intensity value at baseline. Considering this, intensity value measurement in our study should be normalized. Therefore, normalized initial rate of intensity change ( $R$ ) within 5 minutes period was defined as:

$$R = \frac{I_g - I_b}{I_b} \quad (2)$$

Where  $I_g$  represented the detected fluorescence intensity when biosensor was exposed to glucose working solution with difference concentrations;  $I_b$  represented the detected fluorescence intensity when biosensor was exposed to standard buffer solution. In our work, the duration time was taken as 5 minutes because a linear relationship was present (in Figure 6 (c)) in all these response curves. The relationship between initial reaction rates (slopes) within 5 minutes and glucose concentrations was later plotted in Figure 7.

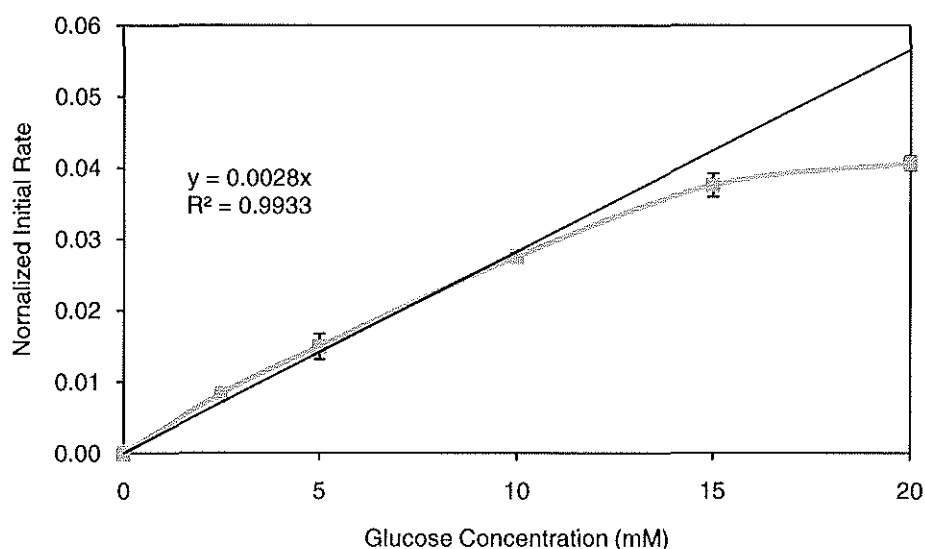


Figure 7 Rate of initial intensity change rate as a function of glucose concentrations (PBS solution, pH=7.42 ± 0.1, duration time =5 min).

In Figure 7, the bulk glucose concentration is ranging from 0 mM to 20 mM. This calibration curve demonstrated an increase tendency of normalized initial rate with the increase of glucose testing solution. At glucose concentration of 0 ~10 mM, a favorable

linear relationship was demonstrated (correlation coefficient: 0.9933,  $y = 0.028x$ ). The initial reaction rate within 5 minutes tended to increase minimally when glucose concentration was at high level.

### 3.3 The effect of GOD concentrations

The concentration of enzyme inside the sensing element was an important parameter for optimization of sensor performance. Figure 8 contained data from experiment in which the enzyme concentrations were varied while holding other reaction parameters constant. Three batches of microfluidic channels were fabricated with three different GOD concentrations (0.012 mM/ml PEGDA, 0.033 mM/ml PEGDA, and 0.056 mM/ml PEGDA). Each batch contained three channels integrated with sensing element at the same enzyme level. It was found that channels in the same batch had similar response curves and corresponding value of normalized reaction rate was averaged and plotted in Figure 8. In order to achieve accurate results, glucose measurements for five different concentrations were conducted three times for each channel.

From calibration curves in Figure 8; it was observed that the sensitivity of glucose sensor increased with the increase of GOD concentrations. However, the linear ranges of these curves were in a reverse trend. This is understandable. Generally, enzyme concentration is positively related to the initial reaction rate while is inversely proportional to apparent Michaelis constant if the glucose and oxygen level is fixed [13]. Therefore, higher enzyme concentration would lead to higher sensitivity but resulted in a narrow glucose measurement range on calibration curve. In our study, since this fluorescent glucose microfluidic sensor was designed for the potential use of human blood glucose level measurement, a reliable glucose sensor should respond linearly up to 10 mM. Therefore, 0.033 mM/ml PEGDA was considered as optimal enzyme concentration since a linear range approximately from 0 mM to 10 mM was demonstrated on this calibration curve with relative high sensitivity.

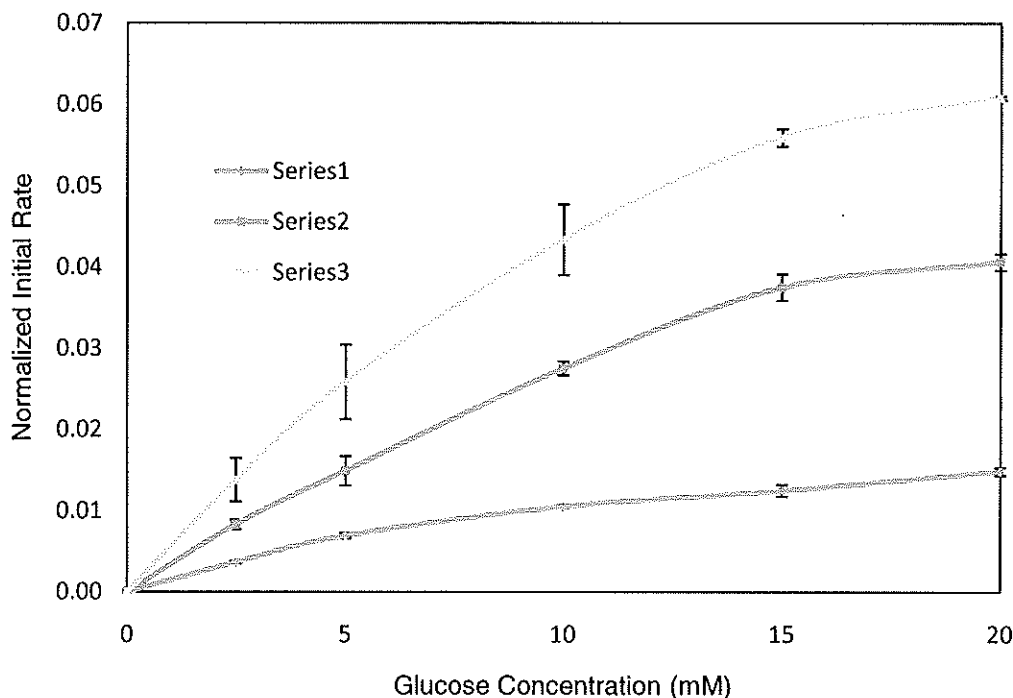


Figure 8 The effect of GOD concentrations on normalized initial rate (Series 1: [GOD]= 0.012mM/ ml PEGDA, n=9; Series 2: [GOD]= 0.033 mM/ ml PEGDA, n=9; Series 3: [GOD]= 0.056 mM/ ml PEGDA, n=6).

### 3.4 Reversibility and repeatability

Figure 6(a) also shows reversibility of the sensor system for glucose measurement. Measurements were performed for the microfluidic sensor integrated with sensing element at enzyme level of 0.033 mM/ml PEGDA. This glucose sensor was alternatively exposed to buffer solution and glucose testing solutions with five different concentrations. As shown in this figure, the fluorescent intensity can return back to the initial signal or baseline after buffer solution was injected into the channels. Good repeatability is also demonstrated by nine times measurements on three different channels (with the same enzyme concentration). Similar calibration curves were achieved with standard deviation no more than 1.8%.

#### 4. CONCLUSIONS

An enzyme-based fluorescent microfluidic glucose sensor with an in-device glucose sensing element was successfully demonstrated. The channel was prepared by utilizing PerMX DFR as the main structural material and PEG monomers, mixed with ruthenium complex and GOD, were filled into the microfluidic channel and lithographically patterned to form a sensing element inside the channel. During glucose measurement, the change of local oxygen level of sensing element was monitored by detecting the change of fluorescent intensity.

In place of the steady-state method, a differential method was proposed here since the reaction inside the sensing element occurred rather slowly. Thus, normalized initial oxygen consumption rates at early stage of glucose reaction were calculated and utilized as an indication of glucose concentrations. The optimal enzyme concentration inside PEG-based sensing element was found out to be 0.033 mM/ml PEGDA since linear detection range of glucose from 0 mM to 10 mM was demonstrated with good sensitivity. Reversibility and repeatability of these sensors were also investigated.

These results indicate that the potential use of fluorescent glucose sensor to monitor blood glucose level by diabetes patients since it responds linearly up to 10 mM (200 mg/dl).

**REFERENCES**

- [1] Moschou E. A., Sharma B. V., Deo S. K., Daunert S., Fluorescence glucose detection: advances toward the ideal in vivo biosensor. *J of Fluoresc.* Sep. 14(5) (2004) 535-547.
- [2] O' Neal D. P., Meledeo M. A., Davis J. R., B. L. Ibey, V. A. Gant, M. V. Pishko, Oxygen sensor based on the fluorescence quenching of a ruthenium complex immobilized in a biocompatible poly(ethylene glycol) hydrogel. *IEEE Sens. J.* 4 (2004) 728-734.
- [3] Mills A., Optical oxygen sensors: utilizing the luminescence of platinum metals complexes. *Platinum Met. Rev.* 41 (1997) 115-127.
- [4] Lakowicz J. R., Chapter 9: Advanced topics in fluorescence quenching. In *Principles of Fluorescence Spectroscopy*. 2nd ed. New York: Plenum, 1999.
- [5] Wolfbeis O. S., Oehme I., Papkovskaya N., Klimant I., Sol-gel based glucose biosensor employing optical oxygen transducers, and a method for compensating for variable oxygen background. *Biosens. Bioelectron.* 15 (2000) 69-76.
- [6] Brown J. Q., Srivastava R., McShane M. J., Encapsulation of glucose oxidase and an oxygen-quenched fluorophore in polyelectrolyte-coated calcium alginate microspheres as optical glucose sensor systems. *Biosens. Bioelectron.* 21 (2005) 212-216.
- [7] Moreno-Bondi M. C., M. Leiner J. P., Schaffar B. P. H., Wolfbeis O. S., Oxygen optrode for use in a fiber-optic glucose biosensor. *Anal. Chem.* 62 (1990) 2377-2380.
- [8] Abgrall, P., Conedera V., Camon H., Gue A-M, Nguyen, N-T, Review: SU-8 as a structural material for labs-on-chips and microelectromechanical systems, *Electrophoresis*, 28 (2007) 4539-4551.
- [9] Makamba H., Kim J. H., Lim K., Park N., Hahn J. H., Surface modification of poly (dimethylsiloxane) (PDMS) microchannels. *Electrophoresis*. 24 (2003) 3607-3619.
- [10] Gao Z., Henthorn D. B., Kim C-S, Enhanced wettability of an SU-8 photoresist through a photografting procedure for bioanalytical device applications. *J. Micromech. Microeng.* 18 (2008) 045013 (7pp).
- [11] Chung C. K., Hong Y. Z., Surface modification of SU-8 photoresist for shrinkage improvement in a monolithic MEMS microstructure. *J. Micromech. Microeng.* 17 (2007) 207-212.

- [12] Vulto P., Glade N., Altomare L., Babet J., Tin L. D., Medoro G., Chartier I., Manaresi, N., Tartagni M., Guerrieri R., Microfluidic channel fabrication in dry film resist for production and prototyping of hybrid chips. *Lab on a chip*. 5 (2005) 158-162.
- [13] Zimmermann S., Fienbork D., Flounders A. W., Liepmann D., In-device enzyme immobilization: wafer-level fabrication of an integrated glucose sensor. *Sens. Actuators. B*. 99 (2004) 163-173.
- [14] Gao Z, Kim C-S, Henthorn D. B., Sensor application of poly (ethylene glycol) diacrylate hydrogels chemically anchored on polymer surface. *Sens. Actuators. B*. (Ready to be submitted).
- [15] Laidler K. J. Bunting P. S., Chapter 2: General kinetic principles. *The Chemical Kinetics of Enzyme Reaction*. 2nd ed. Oxford: Clarendon Press, 35-38.
- [16] Yang, X. F., Zhou Z., Xiao, D., Choi, M. M. F., A fluorescent glucose biosensor based on immobilized glucose oxidase on bamboo inner shell membrane. *Biosens. Bioelectron*. 21 (2006) 1613-1620.

APPENDIX A

DETAILED PROCEDURES FOR SU-8 CHANNEL FABRICATION AND OXYGEN  
SENSING ELEMENTS

Table 1. Fabrication process for bonded monolithic SU-8 channel

Process	Used chemicals/Equipment	Procedure
1 <sup>st</sup> SU-8 layer (bottom layer)		
SU-8 spin-coating step	SU-8 2050 (MicroChem)/ A single wafer spin processor (WS-400E-6NPP/LITE, Lauell Technologies Corporation)	- Spin-coating SU-8 at 500 rpm for 10 seconds, followed by 2000 rpm for 30 seconds to form 75 $\mu\text{m}$ thick layer
Soft-bake process	Hot plate	-Baking at 65 °C for 3 minutes and then at 95 °C for 9 minutes
Exposure	Mask aligner (CA-800, Cobilt)	- UV dose of 330 $\text{mJ}/\text{cm}^2$
Hard-bake process	Hot plate	-Baking at 95 °C for 9 minutes
2 <sup>nd</sup> SU-8 layer (channel structure)		
SU-8 spin-coating step	SU-8 2050 (MicroChem)/ A single wafer spin processor (WS-400E-6NPP/LITE, Lauell Technologies Corporation)	-Spin-coating SU-8 at 500 rpm for 10 seconds, followed by 1000 rpm for 30 seconds to form 12575 $\mu\text{m}$ thick layer
Soft-bake process	Hot plate	-Baking at 95 °C for 10 minutes
Exposure	Mask aligner (CA-800, Cobilt)	-UV dose of 484 $\text{mJ}/\text{cm}^2$
Hard-bake process	Hot plate	-Baking at 95 °C for 9 minutes
Development	Developer (PGMEA, Microchem)/ Isopropanol (Fisher Scientific)	-Soaking in PGMEA for 7 minutes -Use isopropanol to check residue
3 <sup>rd</sup> SU-8 layer (top layer)		
SU-8 spin-coating step	SU-8 2007 (SU-8 2050 diluted by thinner )/A single wafer spin processor (WS-400E- 6NPP/LITE, Lauell Technologies Corporation)	-Spin-coating SU-8 2007 at 500 rpm for 10 seconds, followed by by 2000 rpm for 30 seconds to form 20 $\mu\text{m}$ thick layer
Soft-bake process	Hot plate	-Baking at 95 °C for 4 minutes
Inlet and outlet holes	Drill (Model 750, Dremel)	-Drill holes
Bonding step		
Channel bonding	Hot plate	-Bonding the top and bottom structure at 65 °C for 5 minutes at moderate pressure

Table 2. Chemical anchoring procedure for the PEG-based oxygen sensing element

Process	Used chemicals/Equipments	Procedure
Initiation step	5% (w/w) HCPK solution/ Mask aligner instrument (Karl Suss MA6, Suss MicroTech)/5 ml Syringe	-HCPK solution was bubbled for 30 minutes, then injected into channel - UV dose of 10260 mJ/cm <sup>2</sup>
Washing step	Ethanol /5 ml Syringe	-Residue was washed out by injected ethanol into the channel
Precursor solution preparation	Dichlorotris (1, 10-phenanthroline) ruthenium (II) hydrate 98% (Sigma Aldrich), PEG diacrylate (Mn=575) (Sigma Aldrich), methanol, toluene, D.I. water	-PEGDA: 5ml -Ruthenium complex: 0.01 g -Methanol: 0.065 ml -Toluene: 0.033 ml -D. I. water: 3.8 ml
Pre-polymerization step	Nitrogen gas/ 5 ml syringe	-Precursor solution was bubbled with nitrogen for 30 minutes -Injecting solution into channel
Exposure	Mask aligner instrument (Karl Suss MA6, Suss MicroTech)	-UV dose of 10260 mJ/cm <sup>2</sup>
Washing	D. I. water / 5ml Syringe	-Washing uncrosslinked precursor solution out of channel by injecting D. I. water

## APPENDIX B

### DETAILED PROCEDURES FOR PerMX CHANNEL FABRICATION AND GLUCOSE SENSING ELEMENTS

Table 1. PerMX 3000 series DFR for the fabrication of monolithic microfluidic channel

Process	Used chemicals & equipments	Procedure
1 <sup>st</sup> layer of PerMX (top layer)		
PerMX lamination	DFR (PerMX 3050, DuPont)/ Thermal lamination instrument (TL901, 3M Stationery Products Division)	-Laminating DFR by using thermal lamination instrument -Repeating for 1 layers to obtain 50 $\mu\text{m}$ thick
PerMX post- lamination bake	Hot plate	-Baking at 95 °C for 4 minutes
Exposure	Mask aligner instrument (Karl Suss MA6, Suss MicroTech) with Mask #1	-UV dose of 675 $\text{mJ}/\text{cm}^2$
PerMX post- exposure bake	Hot plate	-Baking at 95 °C for 4 minutes
2 <sup>nd</sup> & 3 <sup>rd</sup> layer of PerMX (channel structure)		
PerMX lamination	DFR (PerMX 3050, DuPont)/ Thermal lamination instrument (TL901, 3M Stationery Products Division)	-Laminating DFR by using thermal lamination instrument -Repeating for 2 layers to obtain 100 $\mu\text{m}$ thick
PerMX post- lamination bake	Hot plate	-Baking at 95 °C for 4 minutes
Exposure	Mask aligner instrument (Karl Suss MA6, Suss MicroTech) with Mask #2	-UV dose of 1012 $\text{mJ}/\text{cm}^2$
PerMX post- exposure bake	Hot plate	-Baking at 95 °C for 8 minutes
Development	Developer (PGMEA, Microchem)/ Isopropanol (Fisher Scientific)	-Soak in PGMEA solution for 9 minutes -Use isopropanol to check the residue
4 <sup>th</sup> layer of PerMX (bottom layer)		
PerMX lamination	DFR (PerMX 3050, DuPont)/ Thermal lamination instrument (TL901, 3M Stationery Products Division)	-Laminating DFR by using thermal lamination instrument -Repeating for 1 layers to obtain 50 $\mu\text{m}$ thick
PerMX post- lamination bake	Hot plate	-Baking at 95 °C for 4 minutes
Bonding step		
Channel bonding	Hot plate	-Bonding the top and bottom structure at 65 °C for 1 minute at moderate pressure

Table 2. Photopatterning procedure for the PEG-based glucose sensing element

Process	Used chemicals/Equipments	Procedure
Precursor solution preparation	Dichlorotris(1,10-phenanthroline) ruthenium (II) hydrate 98% (Sigma Aldrich) /PEG diacrylate (Mn= 575) (Sigma Aldrich)/ photoinitiator (Darocur 1173, Ciba)/ activated GOD solution	- PEGDA: 5ml - Ru complex: 0.002g/ ml PEGDA - Activated GOD solution: 2 ml / ml PEGDA - Photoinitiator: 20 mg/ ml PEGDA
Pre-exposure step	Magnetic stirrer/ Nitrogen gas	-Precursor solution was stirred for 1 hour -Bubbling nitrogen gas for 30 minutes
Precursor solution injection	5 ml Syringe	-Injecting precursor solution into a fluidic chamber
Exposure	Mask aligner instrument (Karl Suss MA6, Suss MicroTech) with Mask #3	-UV dose of 675 mJ/cm <sup>2</sup>
Washing	PBS/ 5 ml Syringe	-Washing uncrosslinked precursor solution out of channel with injecting PBS

### VITA

Zhan Gao was born on November 20, 1981 in Suzhou, China. In June 2004, she received her Bachelor of Engineering degree in Biological and Chemical Engineering department from Nanjing University of Technology, Nanjing, China. She enrolled at Missouri University of Science and Technology (formerly University of Missouri-Rolla) in August 2005 to pursue her Ph.D. degree under the guidance of Dr. David B. Henthorn, Department of Chemical and Biological Engineering. She received her Ph.D degree in May 2011.